J. Fluid Mech. © Cambridge University Press 2012
Supplementary material accompanying doi:10.1017/jfm.2012.126

Analytical linear theory for the shock and re-shock of isotropic density inhomogeneities -Supplementary material-

C. HUETE[1]†, J.G. WOUCHUK[1]
B. CANAUD[2]
A.L. VELIKOVICH[3]

[1]E.T.S.I.I., Instituto de Investigaciones Energéticas (INEI), Universidad de Castilla La Mancha, Campus s/n, 13071 Ciudad Real, Spain
[2]CEA, DAM, DIF, F-91297 Arpajon, France
[3]Plasma Physics Division, NRL, Washington, DC 20375, USA

(Received 25 July 2011; revised 30 December 2011; accepted 1 March 2012)

Appendix A. Introduction

In this Appendix, we show the mathematical formulas and the explanations necessary to make the main text self-contained. It is structured as follows: in Appendix B, we show the results that concern the interaction of a first shock wave with a single mode steady density field. The asymptotic expressions for the different modes downstream are shown. In Appendix C, the interaction of a second shock wave with the perturbations generated by the first shock is discussed. In Appendix D, we show a comparison between the far field perturbations obtained in Appendix C and the transient state solutions provided by a linear numerical code. In Appendix E we discuss the interference between the different mechanism of vorticity generation when a shock wave travels through a density entropy/vorticity perturbation field. For the hypothetic case of suitably chosen perturbation amplitudes upstream, the vorticity or entropy fields downstream might be canceled out. In Appendix F, the different asymptotic limits for the re-shock interacting with a 3D isotropic density spectrum are shown. These limits are obtained for very strong shocks $M_1 \gg 1, M_1' \gg 1$ traveling into a highly compressible gas $\gamma - 1 \ll 1$, or gases with high adiabatic index $\gamma \gg 1$. Finally, in Appendix G we provide some tables of the averaged quantities of interest (kinetic energy, acoustic energy flux, vorticity and density perturbations) either for 2D or 3D, and for different values of γ and shock strengths M_1, M_1'.

Appendix B. First shock/density field interaction

At first, we recast some recently published results concerning the single mode shock-density interaction (Huete Ruiz de Lira *et al.* 2011), which are necessary to address the interaction with a second shock. Before the first shock enters into the perturbed region $x_1 > 0$, the zero-order conservation equations (mass, momentum and energy) across the shock lead to the Rankine-Hugoniot (RH) relationships:

$$R = \frac{\rho_2}{\rho_1} = \frac{D}{D-U} = \frac{(\gamma+1)M_1^2}{(\gamma-1)M_1^2+2}\ , \tag{B 1}$$

† Email address for correspondence: cesar.huete@uclm.es

$$M_2 = \frac{D-U}{c_2} = \sqrt{\frac{(\gamma-1)M_1^2+2}{2\gamma M_1^2-\gamma+1}}\ , \tag{B 2}$$

$$\frac{p_2}{p_1} = \frac{2\gamma M_1^2-\gamma+1}{\gamma+1}\ , \tag{B 3}$$

$$\frac{c_2}{c_1} = \frac{\sqrt{(2\gamma M_1^2-\gamma+1)[(\gamma-1)M_1^2+2]}}{(\gamma+1)M_1}\ , \tag{B 4}$$

where, γ is the gas compressibility, and ρ_i, p_i and c_i refer to the density, pressure and speed of sound ahead of the shock wave ($i=1$) or behind it ($i=2$). The upstream and downstream shock Mach numbers are denoted by M_1 and M_2 respectively. The factor R is the density jump across the shock.

The perturbed density field ($x_1 > 0$) is described as $\rho_1 + \delta\rho_1$ where $\delta\rho_1(x_1, y) = \rho_1\epsilon_k \cos(k_x x_1)\cos(k_y y)$, and the amplitude of the perturbations is $\epsilon_k \ll 1$. Behind the first corrugated shock, density, pressure and velocity fluctuations are created downstream. We define the following dimensionless perturbation functions, factoring out the small parameter ϵ_k:

$$\begin{aligned}
\frac{\delta\rho_2}{\rho_2} &= \epsilon_k\tilde{\rho}_2(x_2,t)\cos(k_y y)\ ,\\
\frac{\delta p_2}{\rho_2 c_2^2} &= \epsilon_k\tilde{p}_2(x_2,t)\cos(k_y y)\ ,\\
\frac{\delta v_{2x}}{c_2} &= \epsilon_k\tilde{v}_{2x}(x_2,t)\cos(k_y y)\ ,\\
\frac{\delta v_{2y}}{c_2} &= \epsilon_k\tilde{v}_{2y}(x_2,t)\sin(k_y y)\ .
\end{aligned} \tag{B 5}$$

In Eq.(B 5), t is the time, and x_2 is the longitudinal coordinate measured in the compressed fluid reference frame (co-moving with the compressed fluid). It is convenient to express the downstream perturbed equations in the compressed reference frame. The quantities $\tilde{v}_{2x}$ and $\tilde{v}_{2y}$ correspond to the longitudinal and transverse velocity fluctuations respectively, and $\tilde{\rho}_2$ and $\tilde{p}_2$ represent the dimensionless density and pressure perturbations. We also define the dimensionless time as $\tau_2 = k_y c_2 t$. The linearized mass, x-momentum and y-momentum conservation equations are, respectively:

$$\begin{aligned}
\frac{\partial\tilde{\rho}_2}{\partial\tau_2} &= -\frac{\partial\tilde{v}_{2x}}{\partial\,(k_y\ x_2)} - \tilde{v}_{2y}\ ,\\
\frac{\partial\tilde{v}_{2x}}{\partial\tau_2} &= -\frac{\partial\tilde{p}_2}{\partial\,(k_y\ x_2)}\ ,\\
\frac{\partial\tilde{v}_{2y}}{\partial\tau_2} &= \tilde{p}_2\ ,
\end{aligned} \tag{B 6}$$

besides, we assume adiabatic flow behind the first shock, which is written as:

$$\frac{\partial\tilde{p}_2}{\partial\tau_2} = \frac{\partial\tilde{\rho}_2}{\partial\tau_2}\ . \tag{B 7}$$

Combining Eqs.(B 6) and using Eq.(B 7), we derive the pressure wave equation:

$$\frac{\partial^2\tilde{p}_2}{\partial\tau_2^2} = \frac{\partial^2\tilde{p}_2}{\partial(k_y x_2)^2} - \tilde{p}_2\ . \tag{B 8}$$

To solve the above wave equation, we need the boundary and initial conditions. In our

case, we suppose that the shock wave travels isolated, which means that there are no waves reaching the shock surface from behind (Huete Ruiz de Lira *et al.* 2011). The other boundary condition is obtained after linearizing the RH relationships [Eqs.(B 1)-(B 4)] and using the continuity of the tangential velocity. In linear theory, the time asymptotic evolution of the perturbed quantities (pressure, density, velocity) does not depend on the initial conditions. We write the linearized RH equations and the tangential velocity conservation for the density/entropy pre-shock modulation ahead of the shock:

$$\frac{d\xi_s}{d\tau_2} = \frac{\gamma+1}{4M_2}\tilde{p}_2 - \frac{M_2 R}{2}\epsilon_k \cos\left(Rk_x x\right) , \tag{B 9}$$

$$\tilde{v}_{2x} = \frac{M_1^2+1}{2M_1^2 M_2}\tilde{p}_2 - \frac{M_2(R-1)}{2}\epsilon_k \cos\left(Rk_x x\right) , \tag{B 10}$$

$$\tilde{v}_{2y} = M_2(R-1)\xi_s , \tag{B 11}$$

$$\tilde{\rho}_2 = \frac{1}{M_1^2 M_2^2}\tilde{p}_2 + \epsilon_k \cos\left(Rk_x x\right) , \tag{B 12}$$

where Eq.(B 9) represents the mass conservation, Eqs.(B 10) and (B 11) correspond to the longitudinal and transverse momentum conservation respectively, and Eq.(B 12) is the energy equation. Here, $\xi_{2s}\epsilon_k = k_y\psi_s$ is the dimensionless shock ripple amplitude. We solve the wave equation with the boundary conditions inside the compressed fluid using the coordinates transformation suggested in (Zaidel' 1960):

$$\begin{aligned} k_y x_2 &= r_2 \sinh\chi_2 , \\ \tau_2 &= r_2 \cosh\chi_2 , \end{aligned} \tag{B 13}$$

here, $\chi_2 = const$ represents a planar front defined by $x_2 = c_2 t \tanh\chi_2$. The shock front coordinate is therefore given by: $\tanh\chi_{2s} = M_2$, and we see that:

$$r_{2s} = \tau_2\sqrt{1-M_2^2} . \tag{B 14}$$

It is convenient to follow the calculations shown in (Wouchuk 2001). We define the auxiliary function $\tilde{h}_2$:

$$\tilde{h}_2 = \frac{1}{r_2}\frac{\partial\tilde{p}_2}{\partial\chi_2} , \tag{B 15}$$

and the wave equation [Eq.(B 8)] for the pressure perturbations is now rewritten as:

$$r_2\frac{\partial^2\tilde{p}_2}{\partial r_2^2} + \frac{\partial\tilde{p}_2}{\partial r_2} + r_2\tilde{p}_2 = \frac{\partial\tilde{h}_2}{\partial\chi_2} . \tag{B 16}$$

We solve the wave equation above with the corresponding boundary conditions a the weak discontinuity ($x_2 = 0$) and at the shock front [$x_2 = x_{2s}(t) = (D-U)t$]. At the shock front [Eqs.(B 9)-(B 12)] can be recast as:

$$\frac{1}{r_{2s}}\frac{\partial\tilde{p}_2}{\partial\chi_2}\Big|_{\chi_{2s}} = -\frac{M_1^2+1}{2M_1^2 M_2}\frac{d\tilde{p}_{2s}}{dr_{2s}} - \frac{M_2^2(R-1)}{\sqrt{1-M_2^2}}\xi_s - \frac{M_2(R-1)}{2}\zeta_0\sin\left(\zeta_0 r_{2s}\right) , \tag{B 17}$$

$$\frac{d\xi_s}{dr_{2s}} = \frac{\gamma+1}{4M_2\sqrt{1-M_2^2}}\tilde{p}_{2s} - \frac{M_2 R}{2\sqrt{1-M_2^2}}\cos\left(\zeta_0 r_{2s}\right) , \tag{B 18}$$

where ζ_0 is the dimensionless frequency that characterizes the periodicity of the pre-shock

density field:

$$\zeta_0 = \frac{RM_2}{\sqrt{1-M_2^2}}\frac{k_x}{k_y} \ . \tag{B 19}$$

We solve Eqs.(B 17)-(B 18) by using the Laplace transform. For any quantity $\varphi(\chi_2, r_2)$ we define its Laplace transform by: $\Phi(\chi_2, s_2) = \int_0^\infty \varphi(\chi_2, r_2)\exp(-s_2 r_2)dr_2$. In particular, for the above shock front equations:

$$H_{2s}(s_2) = -\frac{M_1^2+1}{2M_1^2M_2}\left[s_2P_2(s_2) - \tilde{p}_{20}\right] - \frac{M_2^2(R-1)}{\sqrt{1-M_2^2}}\bar{\xi}_s(s_2) - \frac{M_2(R-1)}{2}\frac{\zeta_0^2}{s_2^2+\zeta_0^2} \ , \tag{B 20}$$

$$s_2\bar{\xi}_s(s_2) - \xi_{s0} = \frac{\gamma+1}{4M_2\sqrt{1-M_2^2}}P_2(s_2) - \frac{M_2R}{2\sqrt{1-M_2^2}}\frac{s_2}{s_2^2+\zeta_0^2} \ , \tag{B 21}$$

where the initial value for the shock pressure $\tilde{p}_{20}$ is obtained with the aid of the conservation equations at $t = 0^+$ between the transmitted shock wave and the reflected sound wave. We get:

$$\tilde{p}_{20} = \frac{M_1^2M_2^2(R-1)}{2M_1^2M_2 + M_1^2 + 1} \ . \tag{B 22}$$

Furthermore, it is clear that the initial shock ripple amplitude is $\xi_{2s0} \equiv 0$, as the shock front is planar in shape when it arrives at $x_2 = 0$. Besides, as discussed in (Velikovich *et al.* 2007; Wouchuk *et al.* 2009), the isolated shock boundary condition is mathematically represented by the relationship: $H_{2s}(s_2) = P_2(s_2)\sqrt{s_2^2+1} - \tilde{p}_{20}$. After some algebra, the exact expression for the Laplace transform of the shock front pressure fluctuations $\tilde{P}_{2s}$ is obtained:

$$\begin{aligned}\tilde{P}_{2s}(s_2) = &\frac{M_1^2M_2^2(R-1)s_2}{2M_1^2M_2s_2\sqrt{s_2^2+1} + (M_1^2+1)\,s_2^2 + M_1^2} + \\ &+ \frac{2M_1^2M_2\alpha_e s_2}{\left[2M_1^2M_2s_2\sqrt{s_2^2+1} + (M_1^2+1)\,s_2^2 + M_1^2\right](s_2^2+\zeta_0^2)} \ .\end{aligned} \tag{B 23}$$

The coefficient α_e characterizes the pre-shock perturbed field:

$$\alpha_e = \frac{M_2(R-1)}{2}\left(\frac{M_2^2R}{1-M_2^2} - \zeta_0^2\right) = \frac{M_1^2 - (M_1^2-1)\zeta_0^2}{\sqrt{(2-M_1^2+\gamma M_1^2)(2\gamma M_1^2+1-\gamma)}} \ . \tag{B 24}$$

Inverting Eq.(B 23), we obtain the shock pressure evolution as a function of the dimensionless time $r_{2s} = \tau_2\sqrt{1-M_2^2}$:

$$\tilde{p}_{2s}(r_{2s}) = \frac{1}{2\pi i}\int_{c-i\infty}^{c+i\infty}\tilde{P}_{2s}(s_2)\exp(s_2r_{2s})ds_2 \ . \tag{B 25}$$

The asymptotic limit of $\tilde{p}_{2s}$ is:

$$\tilde{p}_{2s}(\tau_2 \gg 1) \cong \begin{cases} e_{l1}\cos\left(\frac{k_x}{k_y}RM_2\ \tau_2\right) + e_{l2}\sin\left(\frac{k_x}{k_y}RM_2\ \tau_2\right) & , \ \zeta_0 \le 1 \\ e_s\cos\left(\frac{k_x}{k_y}RM_2\ \tau_2\right) & , \ \zeta_0 \ge 1 \ , \end{cases} \tag{B 26}$$

where the coefficients e_{l1}, e_{l2} and e_s are the same as those obtained in (Velikovich *et al.* 2007; Huete Ruiz de Lira *et al.* 2011):

$$e_{l1} = \frac{2M_1^2M_2\left[M_1^2 - \left(M_1^2+1\right)\zeta_0^2\right]\alpha_e}{4M_1^4M_2^2\zeta_0^2\left(1-\zeta_0^2\right) + \left[M_1^2 - \left(M_1^2+1\right)\zeta_0^2\right]^2} \ ,$$

$$e_{l2} = \frac{4M_1^4 M_2^2 \zeta_0 \sqrt{1-\zeta_0^2}\ \alpha_e}{4M_1^4 M_2^2 \zeta_0^2 (1-\zeta_0^2) + \left[M_1^2 - (M_1^2+1)\,\zeta_0^2\right]^2}\ ,$$
$$e_s = -\frac{2M_1^2 M_2\ \alpha_e}{2M_1^2 M_2 \zeta_0 \sqrt{\zeta_0^2-1} + (M_1^2+1)\,\zeta_0^2 - M_1^2}\ . \tag{B 27}$$

Even though the cases with $\zeta_0 < 1$ (long wavelength regime) and $\zeta_0 > 1$ (short wavelength regime) give rise to different asymptotic behaviors for the pressure field downstream, the expressions shown in Eq.(B 26) are continuous functions of ζ_0. However, the pressure asymptotic amplitudes (e_{l1}, e_{l2}, and e_s) are not continuously differentiable at $\zeta_0 = 1$. This last fact will be important when discussing the acoustic energy flux radiated by the second shock. As studied in (Wouchuk *et al.* 2009; Huete Ruiz de Lira *et al.* 2011; Huete *et al.* 2012), in the long wavelength regime, the pressure disturbances caused by the shock front are evanescent waves, and the intensity decays exponentially behind the shock front. On the other hand, if $\zeta_0 > 1$ the pressure fluctuations travel as stable sonic fronts. Taking into account the Laplace pressure equation Eq.(B 23) and the isolated shock boundary condition, we see that the Laplace transform for the pressure in the whole compressed fluid $\tilde{P}_2(q_2, \chi_2)$ is governed by the following equation:

$$\tilde{P}_2(q_2, \chi_2) = \frac{\cosh\left[q_2 - (\chi_{2s} - \chi_2)\right]}{\cosh q_2} \tilde{P}_{2s}\left[q_2 - (\chi_{2s} - \chi_2)\right]\ , \tag{B 28}$$

where $q_2 = \sinh s_2$. Thus, in the short wavelength regime, the asymptotic expression for the pressure waves at any position x_2 and any time τ_2 is given by:

$$\tilde{p}(x_2, \tau_2) = e_s\ \cos\left(\zeta_1 \tau_2 - k_{2x}^{ac}\ x_2\right)\ , \tag{B 29}$$

where the dimensionless frequency of the compressed fluid is ζ_1, given by:

$$\zeta_1 = \frac{\zeta_0 - M_2\sqrt{\zeta_0^2 - 1}}{\sqrt{1-M_2^2}}\ . \tag{B 30}$$

We notice that that $\zeta_1 < \zeta_0$ because of the Doppler shift. The longitudinal wave number k_{2x}^{ac} associated to the sonic waves is:

$$\frac{k_{2x}^{ac}}{k_y} = \frac{M_2\zeta_0 - \sqrt{\zeta_0^2 - 1}}{\sqrt{1-M_2^2}}\ . \tag{B 31}$$

From Eq.(B 31) it is easy to see that for $1 \le \zeta_0 \le 1/\sqrt{1-M_2^2}$, the waves are emitted to the right, and travel following the shock front, while for $\zeta_0 > 1/\sqrt{1-M_2^2}$ the sound waves escape to the left. We have seen that the corrugated shock induces pressure perturbations downstream, and it also generates post-shock velocity and density disturbances. Once we have obtained analytically the pressure field behind the first shock, we can calculate the velocity field and the other quantities. In particular, it is interesting to study the unstable growth at the interface $x_2 = 0$. Due to the vorticity created to the right side of the interface, the weak discontinuity is Richtmyer-Meshkov unstable and develops a ripple that grows in time. It is important to know the ripple evolution at $x_2 = 0$ because it will act as an initial condition for the re-shock ripple $\xi_{rs0}(\tau_2)$. When the shock wave crosses the interface, it gets a ripple distortion, and as can be deduced from the linearized RH Eqs.(B 9)-(B 12), a velocity field is generated behind the shock. At $t = 0^+$, the Laplace transform for the normal velocity at the interface $\chi_2 = 0$ is:

$$V_{2x}(s_2 = \sinh q_2, \chi_2 = 0) = \frac{-\cosh(q_2 + \chi_{2s}) P_{2s}(q_2 + \chi_{2s})}{\sinh q_2}\ , \tag{B 32}$$

and the exact temporal evolution is given by:

$$\tilde{v}_{2xi}(\tau_2) = \frac{1}{2\pi i}\int_{c-i\infty}^{c+i\infty} V_{2x}(s_2, \chi_2 = 0)\exp\left(s_2\tau_2\right)ds_2 \ , \tag{B 33}$$

where c is a real number to the right of the singularities of the integrand. On the other hand, the Laplace Transform for the interface ripple $\xi_{2i}(s_2)$ is:

$$\xi_{2i}(s_2) = \frac{\left(M_2^2+1\right)\sqrt{s_2^2+1}s_2 + 2M_2 s_2^2 + M_2}{s_2^2\left[M_2^2\left(s_2^2-\zeta_0^2+1\right)+2M_2 s_2\sqrt{s_2^2+1}+s_2^2+\zeta_0^2\right]}\times$$
$$\times\ \frac{\beta_{00}\left[M_2^2\left(s_2^2-\zeta_0^2+1\right)+2M_2 s_2\sqrt{s_2^2+1}+s_2^2+\zeta_0^2\right]+\beta_{20}}{-\beta_{10}s_2^2+\sqrt{s_2^2+1}s_2-\beta_{11}} \ , \tag{B 34}$$

where the coefficients β_{00}, β_{10}, β_{11} and β_{20} are respectively:

$$\begin{aligned}
\beta_{00} &= \frac{2M_1^2M_2+M_1^2+1}{M_2(2M_1^2M_2^2+4M_1^2+2)}\tilde{p}_{20} \ , \\
\beta_{10} &= -\frac{M_1^2\left(5M_2^2+1\right)+M_2^2+1}{2M_2\left[M_1^2\left(M_2^2+2\right)+1\right]} \ , \\
\beta_{11} &= -\frac{M_1^2\left(2M_2^2+1\right)+M_2^2}{2M_2\left[M_1^2\left(M_2^2+2\right)+1\right]} \ , \\
\beta_{20} &= -\frac{M_1^2\left(M_2^2-1\right)}{M_1^2\left(M_2^2+2\right)+1}\alpha_e \ .
\end{aligned} \tag{B 35}$$

It is important to remark that, if $\zeta_0 > 1/\sqrt{1-M_2^2}$, the acoustic waves emitted by the first shock wave fill the whole space downstream and arrive at the interface. These sound waves put the fluid elements to oscillate with dimensionless frequency ζ_1 further modifying the ripple evolution $\xi_i(\tau_2)$. Thus, the asymptotic ripple interface growth (before the second shock crosses it) can be written as:

$$\xi_i(\tau_2 \gg 1) \cong \begin{cases} \xi_{i0}^{\infty} + \tilde{v}_{2xi}^{\infty}\tau_2 & , \ \zeta_0 \leq \frac{M_2}{1-M_2^2} \\ \\ \xi_{i0}^{\infty} + \tilde{v}_{2xi}^{\infty}\tau_2 - e_s\frac{\sqrt{\zeta_1^2-1}}{\zeta_1^2}\sin\left(\zeta_1\tau_2\right) & , \ \zeta_0 \geq \frac{M_2}{1-M_2^2} \ , \end{cases} \tag{B 36}$$

where the initial value for the asymptotic ripple evolution is $\xi_{i0}^{\infty} = \lim_{s_2\to 0}\frac{d}{ds_2}\left[s_2^2\xi_{2i}(s_2)\right]$, and can be expressed as:

$$\xi_{i0}^{\infty} = \tilde{p}_{20}\frac{\left(M_2^2-1\right)\left(M_1^2-M_2^2\right)\left[M_1^2(2M_2+1)+1\right]}{\left[M_1^2\left(2M_2^2+1\right)+M_2^2\right]^2} + \alpha_e 2M_1^2M_2\left(M_2^2-1\right)\times$$
$$\times\ \frac{M_1^2\left[M_2^4\left(\zeta_0^2-5\right)-M_2^2\left(2\zeta_0^2+1\right)+\zeta_0^2\right]-M_2^6\left(\zeta_0^2-1\right)+M_2^4\left(2\zeta_0^2-3\right)-M_2^2\zeta_0^2}{\left[M_1^2\left(2M_2^2+1\right)+M_2^2\right]^2\left[\zeta_0^2-M_2^2\left(\zeta_0^2-1\right)\right]^2} \ . \tag{B 37}$$

The asymptotic normal velocity, $\tilde{v}_{2xi}^{\infty} = -\cosh\chi_{2s}P_{2s}\left(s_2 = \sinh\chi_{2s}\right)$ is given by:

$$\tilde{v}_{2xi}^{\infty} = \frac{-2M_1^2\left(M_1^2-1\right)\left(\gamma M_1^2+1\right)\sqrt{(\gamma-1)M_1^2+2}}{\left[(2\gamma-1)M_1^4+2M_1^2+1\right]\left[(M_1^2-1)(\gamma+1)\zeta_0^2+M_1^2+2\right]\sqrt{2\gamma M_1^2-\gamma+1}} \ . \tag{B 38}$$

Between the weak discontinuity and the shock wave, there are velocity, pressure and

entropy perturbations. The shock ripple oscillations have two effects on the downstream velocity field: on one hand, they generate pressure fluctuations [given by Eqs.(B 9)-(B 12)] which create an irrotational velocity field. On the other hand, the shock corrugation adjusts itself to ensure the conservation of tangential momentum across the shock surface. This last process is the mechanism responsible of generating post-shock vorticity. Hence, the velocity field can be decomposed as the sum of the rotational and potential components $\vec{v}_2 = \vec{v}_2^{rot} + \vec{v}_2^{ac}$. Formally speaking, the dimensionless vorticity associated to the rotational velocity perturbations is defined as:

$$\tilde{\vec{\omega}}_2 = \frac{\delta\vec{\omega}_2}{k_y c_2} = \left(\vec{\nabla}_{2D} \times \tilde{\vec{v}}_2\right) , \tag{B 39}$$

where

$$\vec{\nabla}_{2D} = \left(\frac{\partial}{\partial k_y x_2} , \frac{\partial}{\partial k_y y}\right) , \tag{B 40}$$

with $\tilde{\vec{v}}_2 = (\tilde{v}_{2x}, \tilde{v}_{2y})$. In the absence of viscosity, the vorticity remains frozen to the fluid particles, and can be expressed as:

$$\tilde{\omega}_2(x_2) = \Omega_2 \, \tilde{p}_{2s}\left(\tau_2 = \frac{k_y x_2}{M_2}\right) + \Omega_3 \cos\left(R k_x x_2\right) , \tag{B 41}$$

where $\Omega_2 \, \tilde{p}_{2s}$ is the vorticity contribution directly related to the shock curvature, and the second term $\Omega_3 \, \cos\left(R k_x x_2\right)$ takes into account the interaction between the zero order pressure jump at the shock surface and the gradient of the upstream perturbed density profile. We realize that both terms appear naturally together as a consequence of the conservation of the tangential velocity. They are also written in (Huete Ruiz de Lira *et al.* 2011):

$$\Omega_2 = \frac{\left(M_1^2 - 1\right)^2 \sqrt{2\gamma M_1^2 - \gamma + 1}}{M_1^2 \left[\left(\gamma - 1\right) M_1^2 + 2\right]^{3/2}} , \tag{B 42}$$

$$\Omega_3 = -\frac{M_2 (R^2 - 1)}{2} . \tag{B 43}$$

The asymptotic downstream vorticity is expressed as a piecewise function of ζ_0:

$$\tilde{\omega}_2(x_2 \gg \lambda_y) \cong \begin{cases} \sqrt{\left(\Omega_3 + \Omega_2 e_{l1}\right)^2 + \left(\Omega_2 e_{l2}\right)^2} \cos\left(R k_x x_2 - \phi_{rot}\right) & , \; \zeta_0 \leq 1 \\ \left(\Omega_3 + \Omega_2 e_s\right) \cos\left(R k_x x_2\right) & , \; \zeta_0 \geq 1 \; , \end{cases} \tag{B 44}$$

where $\tan\phi_{rot}$ is given by:

$$\tan\phi_{rot} = \frac{\Omega_2 e_{l2}}{\Omega_3 + \Omega_2 e_{l1}} . \tag{B 45}$$

The far field expressions of the rotational velocity components are:

$$\tilde{v}_{2x}^{rot}(x_2 \gg \lambda_y) \cong \begin{cases} Q_{rot}^l \cos\left(R k_x x_2 - \phi_{rot}\right) & , \; \zeta_0 \leq 1 \\ Q_{rot}^s \cos\left(R k_x x_2\right) & , \; \zeta_0 \geq 1 \; , \end{cases} \tag{B 46}$$

$$\tilde{v}_{2y}^{rot}(x_2 \gg \lambda_y) \cong R\frac{k_x}{k_y} \begin{cases} Q_{rot}^l \sin\left(R k_x x_2 - \phi_{rot}\right) & , \; \zeta_0 \leq 1 \\ Q_{rot}^s \sin\left(R k_x x_2\right) & , \; \zeta_0 \geq 1 \; . \end{cases} \tag{B 47}$$

The quantities Q_{rot}^l and Q_{rot}^s are given by (Huete Ruiz de Lira *et al.* 2011):

$$Q_{rot}^l = -\frac{\sqrt{\left(\Omega_3 + \Omega_2 e_{l1}\right)^2 + \left(\Omega_2 e_{l2}\right)^2}}{1 + \left(R\frac{k_x}{k_y}\right)^2} , \tag{B 48}$$

$$Q^s_{rot} = \frac{\Omega_3 + \Omega_2 e_s}{1 + \left(R\frac{k_x}{k_y}\right)^2} \ . \tag{B 49}$$

Besides the rotational velocity field, there is an acoustic velocity contribution. From the asymptotic pressure field described by Eq.(B 29), and taking into account the Euler equations behind the shock [Eq.(B 10)], we get the acoustic velocity field. We obtain for the longitudinal and transverse components:

$$\tilde{v}^{ac}_{2x}(x_2, \tau_2 \gg 1) = Q_{ac} \cos\left(\zeta_1 \tau_2 - k^{ac}_{2x} x_2\right) \ , \tag{B 50}$$

$$\tilde{v}^{ac}_{2y}(x_3, \tau_2 \gg 1) = \frac{\sqrt{1 - M_2^2}}{M_2\zeta_0 - \sqrt{\zeta_0^2 - 1}} Q_{ac} \sin\left(\zeta_1 \tau_2 - k^{ac}_{2x} x_2\right) \ , \tag{B 51}$$

where:

$$Q_{ac} = \frac{M_2\zeta_0 - \sqrt{\zeta_0^2 - 1}}{\zeta_0 - \sqrt{\zeta_0^2 - 1} M_2} e_s \ . \tag{B 52}$$

The frequencies ζ_1 and k^{ac}_{2x} have been defined in Eqs.(B 30)-(B 31). So far, we have shown the pressure, vorticity and velocity fields generated by the first shock; it also is interesting to know how the density field is modified when the distorted shock travels through this inhomogeneous slab. We decompose the downstream density into the acoustic and entropic contributions:

$$\tilde{\rho}_2(k_y x_2, \tau_2) = \tilde{\rho}^{en}_2(k_y x_2) + \tilde{\rho}^{ac}_2(k_y x_2, \tau_2) \ . \tag{B 53}$$

The acoustic contribution is given by Eq.(B 29):

$$\tilde{\rho}^{ac}_2(k_y x_2, \tau_2) = \tilde{p}_2(k_y x_2, \tau_2) \ , \tag{B 54}$$

and the entropic contribution can be obtained with the aid of RH Eq.(B 12) after subtracting the acoustic part:

$$\tilde{\rho}^{en}_2(k_y x_2) = E_\rho \tilde{p}_{2s}\left(\tau_2 = \frac{k_y x_2}{M_2}\right) + \frac{\delta\rho_1(k_y x_2)}{\rho_1} \ , \tag{B 55}$$

where:

$$E_\rho = \left(\frac{1}{M_1^2 M_2^2} - 1\right) \ . \tag{B 56}$$

At the interface, the entropic field perturbations generated by the first shock are given by:

$$\tilde{\rho}^{en}_{2i} = E_\rho \tilde{p}_{20} + \epsilon_k = \frac{1 - M_1^2 M_1^2 (R-1)}{2M_1^2 M_2 + M_1^2 + 1} \ . \tag{B 57}$$

In the absence of thermal conduction, the entropy perturbations are frozen to the fluid. We use the asymptotic expressions for the shock pressure dynamics to calculate the far field entropic density profile:

$$\tilde{\rho}^{en}_2(x_2 \gg \lambda_y) \cong \begin{cases} Q^l_{en} \cos\left(Rk_x x_2 - \phi_{en}\right) & , \ \zeta_0 \leq 1 \\ Q^s_{en} \cos\left(Rk_x x_2\right) & , \ \zeta_0 \geq 1 \ , \end{cases} \tag{B 58}$$

where the coefficients Q^l_{en} and Q^s_{en} are given by (Huete Ruiz de Lira *et al.* 2011):

$$Q^l_{en} = \sqrt{E_\rho^2 \left(e_{l1}^2 + e_{l2}^2\right) + 2E_\rho e_{l1} + 1} \ , \tag{B 59}$$

$$Q^s_{en} = \sqrt{E_\rho^2 e_s^2 + 2E_\rho e_s + 1} \ , \tag{B 60}$$

and the phase ϕ_{en} is:

$$\tan\phi_{en} = \frac{\left(1 - M_1^2 M_2^2\right) e_{l2}}{M_1^2 M_2^2 + \left(1 - M_1^2 M_2^2\right) e_{l1}} \ . \tag{B 61}$$

In the long wavelength branch ($\zeta_0 < 1$) the vorticity eddies and the entropy spots are spatially shifted because $\phi_{rot} \neq \phi_{en}$. This fact will be important later on, when considering the re-shock of the turbulent field.

Appendix C. Second shock launched into the compressed perturbed fluid

The second shock wave is launched after a time Δt_s following the first shock wave. We assume that the slab length L and the time delay Δt_s are large enough as to ensure that: 1) the sound waves emitted by the first shock have disappeared, and 2) the perturbations left by the first shock have reached their asymptotic regime by the time Δt_s. The details on how L and Δt_s are chosen to meet these constraints have been given in Section 4 of the main article. From here on, we analyze the second shock perturbation dynamics under the assumption that those requirements are met.

Once the second shock enters into the perturbed region ($x_2 > 0$), it reacts generating additional vorticity, entropy, and radiating sound into the re-compressed fluid. We write the conservation equations behind the second shock in the (x_3, y) reference frame (comoving with the re-compressed fluid particles). The linearized mass, x-momentum and y-momentum conservation equations are, respectively:

$$\begin{aligned}
\frac{\partial \tilde{\rho}_3}{\partial \tau_3} &= -\frac{\partial \tilde{v}_{3x}}{\partial\left(k_y\ x_3\right)} - \tilde{v}_{3y}\ , \\
\frac{\partial \tilde{v}_{3x}}{\partial \tau_3} &= -\frac{\partial \tilde{p}_3}{\partial\left(k_y\ x_3\right)}\ , \\
\frac{\partial \tilde{v}_{3y}}{\partial \tau_3} &= \tilde{p}_3\ .
\end{aligned} \tag{C 1}$$

We also assume adiabatic flow behind the second shock, which is represented by:

$$\frac{\partial \tilde{p}_3}{\partial \tau_3} = \frac{\partial \tilde{\rho}_3}{\partial \tau_3}\ . \tag{C 2}$$

Combining Eq.(C 1) and using Eq.(C 2) we get the wave equation for the pressure perturbations downstream of the second shock:

$$\frac{\partial^2 \tilde{p}_3}{\partial \tau_3^2} = \frac{\partial^2 \tilde{p}_3}{\partial (k_y x_3)^2} - \tilde{p}_3\ . \tag{C 3}$$

Our new region of interest is bounded between the second shock and the whole fluid behind (up to $x_3 = 0$). We also adopt here the isolated shock boundary condition assuming that the piston is far enough from the shock. By the time the second shock is launched, only the rotational and entropic perturbations generated by the first shock will affect the second shock perturbation dynamics. Under these assumptions, we write the linearized RH conservation equations and the tangential velocity conservation across the second shock:

$$\frac{d\xi_{rs}}{d\tau_3} = \frac{\gamma+1}{4M_2'}\tilde{p}_3 - \frac{M_2' R'}{2}\frac{\delta\rho_2}{\rho_2} + \frac{M_2' R'}{M_1'}\frac{\delta v_{2x}}{c_2}\ , \tag{C 4}$$

$$\frac{\delta v_{3x}}{c_3} = \frac{M_1'^2+1}{2M_1'^2 M_2'}\tilde{p}_3 - \frac{M_2'(R'-1)}{2}\frac{\delta\rho_2}{\rho_2} + \frac{M_2' R'}{M_1'}\frac{\delta v_{2x}}{c_2} \ , \tag{C 5}$$

$$\frac{\delta\rho_3}{\rho_3} = \frac{1}{M_1'^2 M_2'^2}\tilde{p}_3 + \frac{\delta\rho_2}{\rho_2} \ , \tag{C 6}$$

$$\frac{\delta v_{3y}}{c_3} = M_2'(R'-1)\xi_{rs} \ + \frac{M_2' R'}{M_1'}\frac{\delta v_{2y}}{c_2} \ . \tag{C 7}$$

As we mentioned in the main text, M_1' and M_2' refer to the upstream and downstream second shock Mach numbers, respectively, and R' is the density jump across the second shock. The subscript 3 refers to the re-compressed fluid perturbations. In comparison with Eqs.(B 9)-(B 12), we realize that the rotational velocity field is now added to the upstream perturbed quantities, in the right hand sides of Eqs.(C 4)-(C 7). We also write the relationships between the unperturbed quantities across the second shock, that result from the zero-th order RH equations:

$$R' = \frac{\rho_3}{\rho_2} = \frac{D'}{D'-U'} = \frac{(\gamma+1)M_1'^2}{(\gamma-1)M_1'^2+2} \ , \tag{C 8}$$

$$M_2' = \frac{D'-U'}{c_3} = \sqrt{\frac{(\gamma-1)M_1'^2+2}{2\gamma M_1'^2-\gamma+1}} \ , \tag{C 9}$$

$$\frac{p_3}{p_2} = \frac{2\gamma M_1'^2-\gamma+1}{\gamma+1} \ , \tag{C 10}$$

$$\frac{c_3}{c_2} = \frac{\sqrt{(2\gamma M_1'^2-\gamma+1)[(\gamma-1)M_1'^2+2]}}{(\gamma+1)M_1'} \ . \tag{C 11}$$

The initial conditions for the second shock evolution are given by the initial shock corrugation and the initial shock pressure perturbation. The corrugation is given by the interface corrugation at that time, which is growing due to the RMI [see Eq.(B 36)]. On the other hand, the initial shock pressure is:

$$\tilde{p}_{30} = \frac{M_1'^2 M_2'^2(R'-1)}{2M_1'^2 M_2' + M_1'^2 + M_1'^2}\tilde{\rho}_{2i}^{en} - \frac{2M_1' M_2'^2 R'}{2M_1'^2 M_2' + M_1'^2 + M_1'^2}\tilde{v}_{2xi}^{rot} \ , \tag{C 12}$$

where $\tilde{\rho}_{2i}^{en}$ and $\tilde{v}_{2xi}^{rot}$ correspond to the initial values of entropy [see Eq.(B 57)] and x-velocity [see Eq.(B 38)] respectively generated by first shock at $t = 0^+$. The other boundary condition is given by the second shock wave, and, as it is a moving boundary, the wave equation (C 3) is also solved following the transformation used in Eq.(B 13) (Zaidel' 1960):

$$\begin{aligned} k_y x_3 &= r_3 \sinh\chi_3 \ , \\ \tau_3 &= r_3 \cosh\chi_3 \ . \end{aligned} \tag{C 13}$$

The wave equation [Eq.(C 3)] is rewritten as:

$$r_3^2\frac{\partial^2\tilde{p}_3}{\partial r_3^2} + r_3\frac{\partial\tilde{p}_3}{\partial r_3} + r_3^2\tilde{p}_3 = \frac{\partial^2\tilde{p}_3}{\partial\chi_3^2} \ . \tag{C 14}$$

We also change variables inside the RH equations [Eqs.(C 4)-(C 7)] and get a system of partial differential equations over the variables (r_3, χ_3) that couple $\tilde{p}_3$ and ξ_{rs}. We omit here some of the mathematical details, which are the same as those used in (Wouchuk 2001; Wouchuk *et al.* 2009). To rewrite Eqs.(C 4)-(C 7) using the coordinates (r_3, χ_3), we distinguish between long ($\zeta_0 < 1$) and short ($\zeta_0 > 1$) wavelengths for the vorticity and

entropy fields. The linearized RH equations across the second shock for $\zeta_0 < 1$ are given by:

$$\frac{1}{r_{3s}}\frac{\partial \tilde{p}_3}{\partial \chi_3}\Big|_{\chi_{3s}} = -\frac{M_1'^2+1}{2M_1'^2 M_2'}\frac{d\tilde{p}_{3s}}{dr_{3s}} - \frac{M_2'^2(R'-1)}{\sqrt{1-M_2'^2}}\xi_{rs} + M_2'(R'-1)\zeta_0' \times$$
$$\times \left[\frac{Q_{rot}^l}{M_1'}\sin\left(\zeta_0' r_{3s} - R'\phi_{rot}\right) - \frac{Q_{en}^l}{2}\sin\left(\zeta_0' r_{3s} - R'\phi_{en}\right)\right] , \tag{C 15}$$

$$\frac{d\xi_{rs}}{dr_{3s}} = \frac{\gamma+1}{4M_2'\sqrt{1-M_2'^2}}\tilde{p}_{3s} + Q_{rot}^l \frac{M_2' R'}{M_1'\sqrt{1-M_2'^2}}\cos\left(\zeta_0' r_{3s} - R'\phi_{rot}\right) -$$
$$- Q_{en}^l \frac{M_2' R'}{2\sqrt{1-M_2'^2}}\cos\left(\zeta_0' r_{3s} - R'\phi_{en}\right) , \tag{C 16}$$

and for the short wavelength regime, (noting that now it is $\phi_{en} = \phi_{rot} = 0$) we have:

$$\frac{1}{r_{3s}}\frac{\partial \tilde{p}_3}{\partial \chi_3}\Big|_{\chi_{3s}} = -\frac{M_1'^2+1}{2M_1'^2 M_2'}\frac{d\tilde{p}_{3s}}{dr_{3s}} - \frac{M_2'^2(R'-1)}{\sqrt{1-M_2'^2}}\xi_{rs} +$$
$$+ Q_{rot}^s \frac{M_2'(R'-1)\zeta_0'}{M_1'}\sin\left(\zeta_0' r_{3s}\right) - Q_{en}^s \frac{M_2'(R'-1)\zeta_0'}{2}\sin\left(\zeta_0' r_{3s}\right) , \tag{C 17}$$

$$\frac{d\xi_{rs}}{dr_{3s}} = \frac{\gamma+1}{4M_2'\sqrt{1-M_2'^2}}\tilde{p}_{3s} + Q_{rot}^s \frac{M_2' R'}{M_1'\sqrt{1-M_2'^2}}\cos\left(\zeta_0' r_{3s}\right) -$$
$$- \frac{M_2' R'}{2\sqrt{1-M_2'^2}}\cos\left(\zeta_0' r_{3s}\right) . \tag{C 18}$$

The amplitudes Q_{rot}^l, Q_{rot}^s, Q_{en}^l and Q_{en}^s are the asymptotic amplitudes of the rotational and entropic modes ahead of the second shock, and their values are given in Eqs.(B 48),(B 49),(B 59) and (B 60) respectively. The phases ϕ_{rot} and ϕ_{en} are defined in Eqs.(B 45) and (B 61). We notice that ζ_0' can be expressed as a function of the pre-shock wavenumber vector components, shock intensities (first and second) and the gas compressibility γ [see Eq.(2.2) in the main text]. A distinguishing feature of the re-shock problem is the possibility of generating two branches (long or short wavelength) behind the second shock either for $\zeta_0 < 1$ or $\zeta_0 > 1$. Mathematically, this fact is represented by the two sets of linearized RH equations above. As has been done for the first shock problem, it is convenient to define the derivative pressure function $\tilde{h}_3$ as:

$$\tilde{h}_3 = \frac{1}{r_3}\frac{\partial \tilde{p}_3}{\partial \chi_3} . \tag{C 19}$$

To solve the above differential equations, we also take the Laplace transform, as done in the previous subsection. Equations (C 15)-(C 18) are transformed into an algebraic system. We define the Laplace Transform over the variable r_3 of any quantity ϕ as:

$$\Phi(s_3, \chi_3) = \int_0^\infty \phi(\chi_3, r_3) e^{-s_3 r_3}\, dr_3 . \tag{C 20}$$

Thanks to the isolated shock boundary condition for the second shock, we can see after some algebra that:

$$\tilde{H}_{3s}(s_3) = \tilde{P}_3(s_3)\sqrt{s_3^2+1} - \tilde{p}_{30} . \tag{C 21}$$

Hence, the linearized RH equations at the second shock front can be recast for $\zeta_0 < 1$ as:

$$\tilde{H}_{3s}(s_3) = -\frac{M_1'^2+1}{2M_1'^2M_2'}\left[s_3\tilde{P}_3(s_3) - \tilde{p}_{30}\right] - \frac{M_2'^2(R'-1)}{\sqrt{1-M_2'^2}}\bar{\xi}_{rs}(s_3) + \\ + \quad Q^l_{rot}\frac{M_2'(R'-1)\zeta_0'}{M_1'}\frac{\zeta_0'\cos(R'\phi_{rot}) - s_3\sin(R'\phi_{rot})}{s_3^2+\zeta_0'^2} - \\ - \quad Q^l_{en}\frac{M_2'(R'-1)\zeta_0'}{2}\frac{\zeta_0'\cos(R'\phi_{en}) - s_3\sin(R'\phi_{en})}{s_3^2+\zeta_0'^2}\ , \tag{C 22}$$

$$s_3\bar{\xi}_{rs}(s_3) - \xi_{rs0} = \frac{\gamma+1}{4M_2'\sqrt{1-M_2'^2}}\tilde{P}_3(s_3) + \\ + \quad Q^l_{rot}\frac{M_2'R'}{M_1'\sqrt{1-M_2'^2}}\frac{\zeta_0'\sin(R'\phi_{rot}) + s_3\cos(R'\phi_{rot})}{s_3^2+\zeta_0'^2} - \\ - \quad Q^l_{en}\frac{M_2'R'}{2\sqrt{1-M_2'^2}}\frac{\zeta_0'\sin(R'\phi_{en}) + s_3\cos(R'\phi_{en})}{s_3^2+\zeta_0'^2}\ , \tag{C 23}$$

and for $\zeta_0 > 1$:

$$\tilde{H}_{3s}(s_3) = -\frac{M_1'^2+1}{2M_1'^2M_2'}\left[s_3\tilde{P}_3(s_3) - \tilde{p}_{30}\right] - \frac{M_2'^2(R'-1)}{\sqrt{1-M_2'^2}}\bar{\xi}_{rs}(s_3) + \\ + \quad Q^l_{rot}\frac{M_2'(R'-1)\zeta_0'}{M_1'}'\frac{\zeta_0'}{s_3^2+\zeta_0'^2} - Q^l_{en}\frac{M_2'(R'-1)\zeta_0'}{2}\frac{\zeta_0'}{s_3^2+\zeta_0'^2}\ , \tag{C 24}$$

$$s_3\bar{\xi}_{rs}(s_3) - \xi_{rs0} = \frac{\gamma+1}{4M_2'\sqrt{1-M_2'^2}}\tilde{P}_3(s_3) + \\ + \quad Q^l_{rot}\frac{M_2'R'}{M_1'\sqrt{1-M_2'^2}}\frac{s_3}{s_3^2+\zeta_0'^2} - Q^l_{en}\frac{M_2'R'}{2\sqrt{1-M_2'^2}}\frac{s_3}{s_3^2+\zeta_0'^2}\ . \tag{C 25}$$

From Eqs.(C 22)-(C 25), we obtain an exact and closed expression for the Laplace transform of the pressure perturbations at the second shock [see Eq.(2.3) in the main article]. To obtain the asymptotic expression for the shock pressure dynamics, we study the residues of the shock pressure Laplace transform in Eq.(2.3). In order to study the shock pressure produced by the vorticity ($\tilde{p}^v_{3s}$), and the generated by the entropic field ($\tilde{p}^e_{3s}$), we decompose the pressure behind the shock in the form $\tilde{p}_{3s} = \tilde{p}^v_{3s} + \tilde{p}^e_{3s}$. The asymptotic expression ($r_{3s} \gg 1$) for the vortex-component of the pressure perturbation is:

$$\tilde{p}^v_{3s} \cong \begin{cases} \zeta_0 \le 1 : \frac{Q^l_{rot}}{M_1'} \begin{cases} e_{l1}'\cos(\zeta_0' r_{3s} - R'\phi_{rot}) + e_{l2}'\sin(\zeta_0' r_{3s} - R'\phi_{rot}) & ,\ \zeta_0' \le 1 \\ e_s'\cos(\zeta_0' r_{3s} - R'\phi_{rot}) & ,\ \zeta_0' \ge 1 \end{cases} \\ \zeta_0 \ge 1 : \frac{Q^s_{rot}}{M_1'} \begin{cases} e_{l1}'\cos(\zeta_0' r_{3s}) + e_{l2}'\sin(\zeta_0' r_{3s}) & ,\ \zeta_0' \le 1 \\ e_s'\cos(\zeta_0' r_{3s}) & ,\ \zeta_0' \ge 1\ , \end{cases} \end{cases} \tag{C 26}$$

where we note [see Eqs.(C 13)] that $r_{3s} = \tau_3\sqrt{1-M_2'^2}$. The entropy-component of the pressure perturbation is:

$$\tilde{p}^e_{3s} \cong \begin{cases} \zeta_0 \le 1 : -\frac{Q^l_{en}}{2} \begin{cases} e_{l1}'\cos(\zeta_0' r_{3s} - R'\phi_{en}) + e_{l2}'\sin(\zeta_0' r_{3s} - R'\phi_{en}) & ,\ \zeta_0' \le 1 \\ e_s'\cos(\zeta_0' r_{3s} - R'\phi_{en}) & ,\ \zeta_0' \ge 1 \end{cases} \\ \zeta_0 \ge 1 : -\frac{Q^s_{en}}{2} \begin{cases} e_{l1}'\cos(\zeta_0' r_{3s}) + e_{l2}'\sin(\zeta_0' r_{3s}) & ,\ \zeta_0' \le 1 \\ e_s'\cos(\zeta_0' r_{3s}) & ,\ \zeta_0' \ge 1\ . \end{cases} \end{cases} \tag{C 27}$$

The coefficients e'_{l1}, e'_{l2}, and e'_s are:

$$
\begin{aligned}
e'_{l1} &= \frac{2M_1'^2 M_2' \left[M_1'^2 - \left(M_1'^2+1\right)\zeta_0'^2\right]\alpha'}{4M_1'^4 M_2'^2 \zeta_0'^2\left(1-\zeta_0'^2\right) + \left[M_1'^2 - \left(M_1'^2+1\right)\zeta_0'^2\right]^2} \ , \\
e'_{l2} &= \frac{4M_1'^4 M_2'^2 \zeta_0' \sqrt{1-\zeta_0'^2}\ \alpha'}{4M_1'^4 M_2'^2 \zeta_0'^2\left(1-\zeta_0'^2\right) + \left[M_1'^2 - \left(M_1'^2+1\right)\zeta_0'^2\right]^2} \ , \\
e'_s &= -\frac{2M_1'^2 M_2'\ \alpha'}{2M_1'^2 M_2' \zeta_0' \sqrt{\zeta_0'^2-1} + \left(M_1'^2+1\right)\zeta_0'^2 - M_1'^2} \ ,
\end{aligned}
\tag{C 28}
$$

where α' is:

$$
\alpha' = 2M_1'^2 M_2'^2 (R'-1)\left(\zeta_0'^2 - \frac{M_1'^2}{M_1'^2-1}\right) \ . \tag{C 29}
$$

Both vortical and entropic contributions to the shock pressure evolution can be combined into a single expression, which is given in Eq.(2.4) in the main article and repeated here:

$$
\tilde{p}_{3s}(r_{3s} \gg 1) \cong \begin{cases} \zeta_0 \le 1 : \begin{cases} \pi_{ll1}\cos\left(\ \zeta_0' r_{3s}\ \right) + \pi_{ll2}\sin\left(\ \zeta_0' r_{3s}\ \right) & , \ \zeta_0' \le 1 \\ \pi_{ls1}\cos\left(\ \zeta_0' r_{3s}\ \right) + \pi_{ls2}\sin\left(\ \zeta_0' r_{3s}\ \right) & , \ \zeta_0' \ge 1 \end{cases} \\ \zeta_0 \ge 1 : \begin{cases} \pi_{sl1}\cos\left(\ \zeta_0' r_{3s}\ \right) + \pi_{sl2}\sin\left(\ \zeta_0' r_{3s}\ \right) & , \ \zeta_0' \le 1 \\ \pi_{ss}\cos\left(\ \zeta_0' r_{3s}\ \right) & , \ \zeta_0' \ge 1 \end{cases} \end{cases} ,
$$

where the amplitudes are given by:

$$
\begin{aligned}
\pi_{ll1} &= \frac{Q^l_{rot}}{M_1'}\left[e'_{l1}\cos\left(R'\phi_{rot}\right) - e'_{l2}\sin\left(R'\phi_{rot}\right)\right] - \frac{Q^l_{en}}{2}\left[e'_{l1}\cos\left(R'\phi_{en}\right) - e'_{l2}\sin\left(R'\phi_{en}\right)\right] \ , \\
\pi_{ll2} &= \frac{Q^l_{rot}}{M_1'}\left[e'_{l1}\sin\left(R'\phi_{rot}\right) + e'_{l2}\cos\left(R'\phi_{rot}\right)\right] - \frac{Q^l_{en}}{2}\left[e'_{l1}\sin\left(R'\phi_{en}\right) + e'_{l2}\cos\left(R'\phi_{en}\right)\right] \ , \\
\pi_{ls1} &= \frac{Q^l_{rot}}{M_1'} e'_s \cos\left(R'\phi_{rot}\right) - \frac{Q^l_{en}}{2} e'_s \cos\left(R'\phi_{en}\right) \ , \\
\pi_{ls2} &= \frac{Q^l_{rot}}{M_1'} e'_s \sin\left(R'\phi_{rot}\right) - \frac{Q^l_{en}}{2} e'_s \sin\left(R'\phi_{en}\right) \ , \\
\pi_{sl1} &= \frac{Q^s_{rot}}{M_1'} e'_{l1} - \frac{Q^s_{en}}{2} e'_{l1} \ , \\
\pi_{sl2} &= \frac{Q^s_{rot}}{M_1'} e'_{l2} - \frac{Q^s_{en}}{2} e'_{l2} \ , \\
\pi_{ss} &= \frac{Q^s_{rot}}{M_1'} e'_s - \frac{Q^s_{en}}{2} e'_s \ .
\end{aligned}
\tag{C 30}
$$

As has been shown in the previous section, the Laplace transform for the pressure at any point of the re-compressed fluid is:

$$
\tilde{P}_3(q_3, \chi_3) = \frac{\cosh\left[q_3 - (\chi_{3s} - \chi_3)\right]}{\cosh q_3} \tilde{P}_{3s}\left[q_3 - (\chi_{3s} - \chi_3)\right] \ , \tag{C 31}
$$

where $q_3 = \sinh s_3$ and $0 \le \chi_3 \le \chi_{3s}$. If we substitute $\tilde{P}_{3s}$ from Eq.(2.3) into Eq.(C 31), we notice that we may have new poles at $\pm i\zeta'_\chi$ where $\zeta'_\chi = \cosh\left[\cosh^{-1}\zeta_0' - (\chi_{3s} - \chi_3)\right]$.

In the previous Appendix B, we have seen that the first shock generates a vorticity field behind it, generated by the shock curvature and the baroclinic interaction. In the re-shock problem, where the second shock travels into the perturbed field generated by the first shock, a new vorticity field is generated downstream. We define the dimensionless

vorticity behind the second shock as:

$$\tilde{\vec{\omega}}_3 = \frac{\delta\vec{\omega}_{3z}}{k_y c_3} = \left(\vec{\nabla}_{2D} \times \tilde{\vec{v}}_3\right) , \tag{C 32}$$

where the operator $\vec{\nabla}_{2D}$ is:

$$\vec{\nabla}_{2D} = \left(\frac{\partial}{\partial k_y x_3} , \frac{\partial}{\partial k_y y}\right) . \tag{C 33}$$

The vorticity generation behind the second shock is given in Eq.(2.13) in the main article, and the asymptotic vorticity field is given in Eq.(2.17) and repeated here:

$$\tilde{\omega}_3(x_3 \gg \lambda_y) \cong \begin{cases} \zeta_0 \le 1 : \begin{cases} w_{ll1}\cos(\ R'Rk_x x_3\ ) + w_{ll2}\sin(\ R'Rk_x x_3\ ) & , \ \zeta_0' \le 1 \\ w_{ls1}\cos(\ R'Rk_x x_3\ ) + w_{ls2}\sin(\ R'Rk_x x_3\ ) & , \ \zeta_0' \ge 1 \end{cases} \\ \zeta_0 \ge 1 : \begin{cases} w_{sl1}\cos(\ R'Rk_x x_3\ ) + w_{sl2}\sin(\ R'Rk_x x_3\ ) & , \ \zeta_0' \le 1 \\ w_{ss}\cos(\ R'Rk_x x_3\ ) & , \ \zeta_0' \ge 1 \ . \end{cases} \end{cases}$$

The corresponding amplitudes of the asymptotic mode are:

$$\begin{aligned}
w_{ll1} &= Q^l_{rot}\{\Omega_1'\cos(R'\phi_{rot}) + \frac{\Omega_2'}{M_1'}[e_{l1}\cos(R'\phi_{rot}) - e_{l2}\sin(R'\phi_{rot})]\} + \\
&+ Q^l_{en}\{\Omega_3'\cos(R'\phi_{en}) - \frac{\Omega_2'}{2}[e_{l1}\cos(R'\phi_{en}) - e_{l2}\sin(R'\phi_{en})]\} , \\
w_{ll2} &= Q^l_{rot}\{\Omega_1'\sin(R'\phi_{rot}) + \frac{\Omega_2'}{M_1'}[e_{l1}\sin(R'\phi_{rot}) + e_{l2}\cos(R'\phi_{rot})]\} + \\
&+ Q^l_{en}\{\Omega_3'\sin(R'\phi_{en}) - \frac{\Omega_2'}{2}[e_{l1}\sin(R'\phi_{en}) + e_{l2}\cos(R'\phi_{en})]\} , \\
w_{ls1} &= Q^l_{rot}\left(\Omega_1' + \frac{\Omega_2'}{M_1'}e_s\right)\cos(R'\phi_{rot}) + Q^l_{en}\left(\Omega_3' - \frac{\Omega_2'}{2}e_s\right)\cos(R'\phi_{en}) , \\
w_{ls2} &= Q^l_{rot}\left(\Omega_1' + \frac{\Omega_2'}{M_1'}e_s\right)\sin(R'\phi_{rot}) + Q^l_{en}\left(\Omega_3' - \frac{\Omega_2'}{2}e_s\right)\sin(R'\phi_{en}) , \\
w_{sl1} &= Q^s_{rot}\left(\Omega_1' + \frac{\Omega_2'}{M_1'}e_{l1}\right) + Q^s_{en}\left(\Omega_3' - \frac{\Omega_2'}{2'}e_{l1}\right) , \\
w_{sl2} &= Q^s_{rot}\frac{\Omega_2'}{M_1'}e_{l2} - Q^s_{en}\frac{\Omega_2'}{2}e_{l2} , \\
w_{ss} &= Q^s_{rot}\left(\Omega_1' + \frac{\Omega_2'}{M_1'}e_s\right) + Q^s_{en}\left(\Omega_3' - \frac{\Omega_2'}{2}e_s\right) .
\end{aligned} \tag{C 34}$$

As we did for the second shock pressure perturbation, we separate the vorticity field left by the second shock into the part generated by the vortical structures ahead $\tilde{\omega}_3^v$ and the part due to the entropic spots $\tilde{\omega}_3^e$. Hence, we can study how these contributions interact to create the new total vorticity field behind the second shock. We make $\tilde{\omega}_3 = \tilde{\omega}_3^v + \tilde{\omega}_3^e$, where:

$$\tilde{\omega}_3^v(x_3 \gg \lambda_y) \cong \begin{cases} \zeta_0 \le 1 : \begin{cases} w^v_{ll1}\cos(\ R'Rk_x x_3\ ) + w^v_{ll2}\sin(\ R'Rk_x x_3\ ) & , \ \zeta_0' \le 1 \\ w^v_{ls1}\cos(\ R'Rk_x x_3\ ) + w^v_{ls2}\sin(\ R'Rk_x x_3\ ) & , \ \zeta_0' \ge 1 \end{cases} \\ \zeta_0 \ge 1 : \begin{cases} w^v_{sl1}\cos(\ R'Rk_x x_3\ ) + w^v_{sl2}\sin(\ R'Rk_x x_3\ ) & , \ \zeta_0' \le 1 \\ w^v_{ss}\cos(\ R'Rk_x x_3\ ) & , \ \zeta_0' \ge 1 \ . \end{cases} \end{cases} \tag{C 35}$$

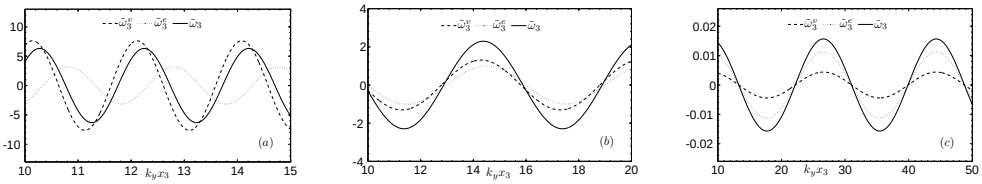

FIGURE 1. Different contributions for the vorticity field left behind the second shock for $M_1 = M_1' = 2.0$, $k_x/k_y = 1/5$, and for $\gamma - 1 \ll 1$, $\zeta_0 \cong 0.462$ (a), $\gamma = 5/3$, $\zeta_0 \cong 0.349$ (b), and $\gamma \gg 1$, $\zeta_0 \cong 0.233$ (c).

$$\tilde{\omega}_3^e(x_3 \gg \lambda_y) \cong \begin{cases} \zeta_0 \leq 1: & \begin{cases} w^e_{ll1}\cos(\,R'Rk_x x_3\,) + w^e_{ll2}\sin(\,R'Rk_x x_3\,) & ,\ \zeta_0' \leq 1 \\ w^e_{ls1}\cos(\,R'Rk_x x_3\,) + w^e_{ls2}\sin(\,R'Rk_x x_3\,) & ,\ \zeta_0' \geq 1 \end{cases} \\ \zeta_0 \geq 1: & \begin{cases} w^e_{sl1}\cos(\,R'Rk_x x_3\,) + w^e_{sl2}\sin(\,R'Rk_x x_3\,) & ,\ \zeta_0' \leq 1 \\ w^e_{ss}\cos(\,R'Rk_x x_3\,) & ,\ \zeta_0' \geq 1\ . \end{cases} \end{cases} \tag{C 36}$$

where the amplitudes w^{rot} and w^e are the part proportional to Q_{rot} and Q_{en} in Eq.(C 34) respectively. We plot both contributions together with the total vorticity field for $M_1 = M_1' = 2$, $k_x/k_y = 1/5$, and different gases in Figure 1. We observe remarkable differences between highly compressible gases $\gamma - 1 \ll 1$, and gases with a higher adiabatic index $\gamma \gg 1$. The phase shift that appears in Figure 1(a) between the entropic and vortical contributions gives rise a negative interference between both terms. In contrast, for the case studied in Figure 1(c), we observe a total positive interference between both contributions. Finally, for a gas with $\gamma = 5/3$, in Figure 1(b) we observe a slight phase shift between both parts. Therefore, the small negative interference is not dominant for monatomic gases under these conditions of shock strengths and upstream mode spatial frequency. The spatial shift only appears outside of the region where $\zeta_0 \geq 1$ and $\zeta_0' \geq 1$ simultaneously.

From the conservation equations (C 1), it can be seen that the velocity perturbation field behind the second shock satisfies the following differential equation:

$$\frac{\partial^2 \tilde{\vec{v}}_3}{\partial \tau_3^2} = \vec{\nabla}_{2D} \times \left(\vec{\nabla}_{2D} \times \tilde{\vec{v}}_3 \right) + \nabla^2_{2D} \tilde{\vec{v}}_3\ . \tag{C 37}$$

As done for the single shock/entropy interaction, the velocity field generated behind the shock is decomposed into rotational and acoustic contributions:

$$\tilde{\vec{v}}_3 = \tilde{\vec{v}}_3^{\,rot} + \tilde{\vec{v}}_3^{\,ac}\ . \tag{C 38}$$

In the absence of viscosity, the rotational mode is steady, and hence, the time dependence disappears in the above Eq.(C 37):

$$\nabla^2_{2D} \tilde{\vec{v}}_3^{\,rot} = -\vec{\nabla}_{2D} \times \left(\vec{\nabla}_{2D} \times \tilde{\vec{v}}_3^{\,rot} \right) = -\vec{\nabla}_{2D} \times \tilde{\vec{\omega}}_3\ . \tag{C 39}$$

The solution of Eq.(C 39) has been shown in Eqs.(2.18)-(2.19). The corresponding amplitudes amplitudes are:

$$\begin{aligned} Q'_{rot,ll} &= -\frac{\sqrt{w^2_{ll1} + w^2_{ll2}}}{1 + \left(\frac{R'Rk_x}{k_y}\right)^2}\ , \qquad Q'_{rot,ls} = -\frac{\sqrt{w^2_{ls1} + w^2_{ls2}}}{1 + \left(\frac{R'Rk_x}{k_y}\right)^2}\ , \\ Q'_{rot,sl} &= -\frac{\sqrt{w^2_{sl1} + w^2_{sl2}}}{1 + \left(\frac{R'Rk_x}{k_y}\right)^2}\ , \qquad Q'_{rot,ss} = \frac{w_{ss}}{1 + \left(\frac{R'Rk_x}{k_y}\right)^2}\ . \end{aligned} \tag{C 40}$$

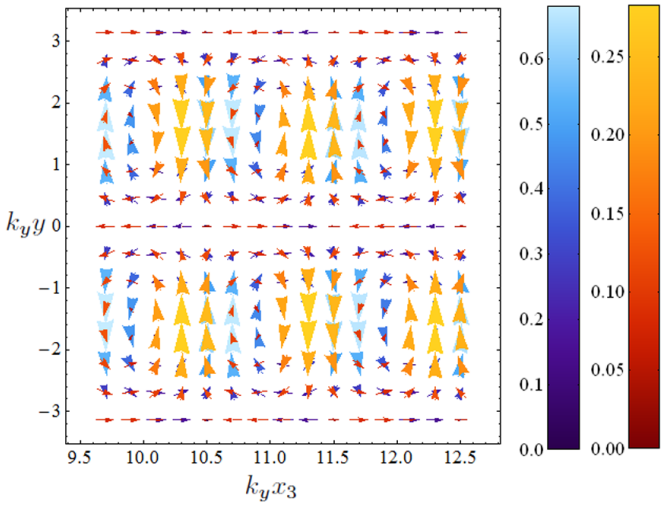

FIGURE 2. Different contributions (entropic and vortical) for the rotational velocity field left behind the second shock for $M_1 = M_1' = 2.0$, $k_x/k_y = 1/5$, $\gamma - 1 << 1$, $\zeta_0 \cong 0.462$.

We recognize new phases associated to the vortical mode in the arguments of Eqs.(2.18)-(2.19), they are:

$$\phi'_{rot,ll} = \tan^{-1}\left(\frac{w_{ll2}}{w_{ll1}}\right) , \qquad \phi'_{rot,ls} = \tan^{-1}\left(\frac{w_{ls2}}{w_{ls1}}\right) ,$$
$$\phi'_{rot,sl} = \tan^{-1}\left(\frac{w_{sl2}}{w_{sl1}}\right) . \tag{C 41}$$

As we did for the vorticity field, it is interesting to separate the rotational velocity field into the components generated by the vortical and entropic perturbations ahead of the second shock. The corresponding values are the same of those shown in Eqs.(C 40)-(C 41), by just replacing w by the corresponding w^v and w^e, as done in Eqs.(C 35)-(C 36). In Figure 2, we plot the vorticity contribution in blue, superposed to the entropic contribution in orange for $M_1 = M_1' = 2.0$, $k_x/k_y = 1/5$, $\gamma - 1 << 1$, ($\zeta_0 \cong 0.462$), which correspond to the same values that those used in Figure 1(a). As happened with the vorticity field, both vortical and entropic contributions interferes negatively to create a downstream rotational velocity field with less kinetic energy.

On the other hand, the acoustic velocity field is governed by the sound wave equation:

$$\frac{\partial^2 \tilde{v}_3^{ac}}{\partial^2 \tau_3^2} = \nabla_{2D}^2 \tilde{v}_3^{ac} . \tag{C 42}$$

In the asymptotic regime, the acoustic velocity field is a piecewise function of ζ_0 as can be seen from Eqs.(2.20)-(2.21) in the main text. The amplitudes $Q'_{ac,l}$ and $Q'_{ac,s}$ are:

$$Q'_{ac,l} = \frac{M_2'\zeta_0' - \sqrt{\zeta_0'^2 - 1}}{\zeta_0' - M_2'\sqrt{\zeta_0'^2 - 1}} \sqrt{\pi_{ls1}^2 + \pi_{ls2}^2} ,$$
$$Q'_{ac,s} = \frac{M_2'\zeta_0' - \sqrt{\zeta_0'^2 - 1}}{\zeta_0' - M_2'\sqrt{\zeta_0'^2 - 1}} \pi_{ss} . \tag{C 43}$$

We remind that, the condition to have stable sound waves behind the second shock, is mathematically given by $\zeta_0' > 1$ [See Eq.(2.2) in the main text].

In Eq.(2.23), the density-entropic field generated behind the second shock is shown, together with the corresponding asymptotic expression [see also Eq.(2.25)]:

$$\tilde{\rho}_3^{en}(x_3 \gg \lambda_y) \cong \begin{cases} \zeta_0 \leq 1: & \begin{cases} Q'_{en,ll}\cos\left(\, R'Rk_x x_3 - \phi'_{en,ll}\,\right) & ,\ \zeta_0' \leq 1 \\ Q'_{en,ls}\cos\left(\, R'Rk_x x_3 - \phi'_{en,ls}\,\right) & ,\ \zeta_0' \geq 1 \end{cases} \\ \zeta_0 \geq 1: & \begin{cases} Q'_{en,sl}\cos\left(\, R'Rk_x x_3 - \phi'_{en,sl}\,\right) & ,\ \zeta_0' \leq 1 \\ Q'_{en,ss}\cos\left(\, R'Rk_x x_3\,\right) & ,\ \zeta_0' \geq 1\ , \end{cases} \end{cases}$$

where the amplitudes are:

$$\begin{aligned} Q'_{en,ll} &= \sqrt{d_{ll1}^2 + d_{ll2}^2}\ , \qquad Q'_{en,ls} = \sqrt{d_{ls1}^2 + d_{ls2}^2}\ , \\ Q'_{en,sl} &= \sqrt{d_{sl1}^2 + d_{sl2}^2}\ , \qquad Q'_{en,ss} = d_{ss}\ . \end{aligned} \tag{C 44}$$

The coefficients d_{ll}, d_{ls}, d_{ss} and d_{ss} are given by:

$$\begin{aligned} d_{ll1} &= Q^l_{rot}\frac{E'_\rho}{M'_1}\left[e'_{l1}\cos\left(R'\phi_{rot}\right) - e'_{l2}\sin\left(R'\phi_{rot}\right)\right] - \\ &\quad - Q^l_{en}\frac{E'_\rho}{2}\left[e'_{l1}\cos\left(R'\phi_{en}\right) - e'_{l2}\sin\left(R'\phi_{en}\right)\right] + Q^l_{en}\cos\left(R'\phi_{en}\right)\ , \\ d_{ll2} &= Q^l_{rot}\frac{E'_\rho}{M'_1}\left[e'_{l1}\sin\left(R'\phi_{rot}\right) + e'_{l2}\cos\left(R'\phi_{rot}\right)\right] - \\ &\quad - Q^l_{en}\frac{E'_\rho}{2}\left[e'_{l1}\sin\left(R'\phi_{en}\right) + e'_{l2}\cos\left(R'\phi_{en}\right)\right] + Q^l_{en}\sin\left(R'\phi_{en}\right)\ , \\ d_{ls1} &= Q^l_{rot}\frac{E'_\rho}{M'_1}e'_s\cos\left(R'\phi_{rot}\right) + Q^l_{en}\left(-\frac{E'_\rho}{2}e'_s + 1\right)\cos\left(R'\phi_{en}\right)\ , \\ d_{ls2} &= Q^l_{rot}\frac{E'_\rho}{M'_1}e'_s\sin\left(R'\phi_{rot}\right) + Q^l_{en}\left(-\frac{E'_\rho}{2}e'_s + 1\right)\sin\left(R'\phi_{en}\right)\ , \\ d_{sl1} &= Q^s_{rot}\frac{E'_\rho}{M'_1}e'_{l1} + Q^s_{en}\left(-\frac{E'_\rho}{2}e'_{l1} + 1\right)\ , \\ d_{sl2} &= Q^s_{rot}\frac{E'_\rho}{M'_1}e'_{l2} + Q^s_{en}\left(-\frac{E'_\rho}{2}e'_{l2} + 1\right)\ , \\ d_{ss} &= Q^s_{rot}\frac{E'_\rho}{M'_1}e'_s + Q^s_{en}\left(-\frac{E'_\rho}{2}e'_s + 1\right)\ , \end{aligned} \tag{C 45}$$

and the phases of the entropy spots are:

$$\begin{aligned} \phi'_{en,ll} &= \tan^{-1}\left(\frac{d_{ll2}}{d_{ll1}}\right)\ , \qquad \phi'_{en,ls} = \tan^{-1}\left(\frac{d_{ls2}}{d_{ls1}}\right)\ , \\ \phi'_{en,sl} &= \tan^{-1}\left(\frac{d_{sl2}}{d_{sl1}}\right)\ . \end{aligned} \tag{C 46}$$

Appendix D. Linear Numerical Simulations

We compare here the analytical results to numerical calculation done with the Linear Perturbative Code (LPC) described in (Morice & Jaouen 2003; Clarisse *et al.* 2004). The

code solves simultaneously the one-dimensional fluid equations for the mean flow and their linearized form for three dimensional perturbations. The set of 3D-linearized equations is reduced to a 1D system for the modal components of the linear perturbation using a Fourier decomposition in the transverse plane in planar geometry. The axial geometry is described by a sinusoidal function $cos(k_x x + \phi)$. A linear Lagrangian perturbation approach is considered here. A Godunov-type scheme including high order extension is used. Heat conduction, radiative transfer and viscosity are neglected, in correspondence with the linear model developed in the previous Appendices B and C. Perfect gas equations of state are used with a polytropic exponent γ. Mesh refinement shows the convergence of calculations. In order to compare the numerical results with the asymptotic analytical functions obtained in the previous section, we set two different shock waves propagating in a row in the same box. As the first shock is subsonic with respect to fluid behind, any subsequent shock will catch up the previous one. This configuration adds a restriction in the second shock strength, because high second Mach numbers M_1' imply that the second shock catches up the first one ahead before the asymptotic regime is achieved. Besides, as we do not consider the interaction between the second shock and the acoustic flux emitted by the first shock front, we only consider the cases in which $\zeta_0 < 1$, in other words, we only compare the numerical cases where the pressure waves emitted by the first shock decay exponentially, and hence, they do not interact with the shock behind. This assumption guarantees that the second shock travels interacting only with the rotational and entropic modes generated by the first one. In that sense, both numerical and analytical results complement each other, because the numerical work allows facing more complex situations and theoretical work provides analytical scaling laws for the whole range of parameters. In Figure 3 we plot two numerical simulations for the density field superposed to the analytical asymptotic behavior predicted by Eqs.(2.25). The perturbations are analyzed in the laboratory system of reference (x_1, y), where the first shock moves with relative shock velocity $D\hat{x}_1$. We see how both shocks amplify the density field and compress the initial entropic longitudinal wavelength (a factor R for the first shock and $R' \cdot R$ for the second shock). For both figures, the shock intensities are $M_1 = 2$ and $M_1' = 1.2$ and the gas has an adiabatic index $\gamma = 5/3$. The upstream density profiles in Figure 3(a) and Figure 3(b) are characterized by $k_x/k_y = 1/5$ and $k_x/k_y = 1/2$ respectively. We observe that there are no acoustic waves emitted by the first shock in any case ($\zeta_0 = 0.349149$ and $\zeta_0 = 0.872872$ respectively). Nevertheless, the characteristic shock oscillations for the second front are $\zeta_0' = 0.941947$, and $\zeta_0' = 2.35487$, respectively, and hence, the second shock emits sonic stable sonic waves in the second case ($\zeta_0' > 1$).

From Figure 3 we notice that the numerical simulations agree very well with the asymptotic theoretical results shown in Appendix C.

Appendix E. Suppression of the downstream rotational or entropic field

We have seen that, for certain conditions, the vorticity generation behind the second shock is given by a negative interference between the different contributions. Therefore, it is natural to think about the possibility of generating an irrotational velocity field downstream. That is, we look for the values of $\gamma, M_1, M_1', k_x/k_y$ which give rise irrotational velocity perturbations behind the second shock. Other authors in the past have also addressed this question (Kevlahan 1997; Azara & Emanuel 1988), and they concluded that the post shock will never be irrotational if the flow ahead is rotational. To study the possibility of irrotational flows downstream, we suggest the hypothetical case

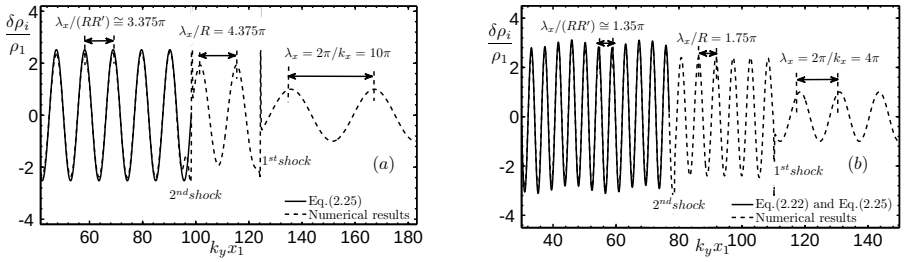

FIGURE 3. (Color Online) In dashed line it is plotted the numerical results for the density perturbed field (ρ_i/ρ_1) in the three zones $(i = 1, 2, 3)$ for $M_1 = 2$ and $M_1' = 1.2$ and $\gamma = 5/3$. In solid black line it is plotted the asymptotic analytical expression. The pre-shock mode in case (a) is $k_x = 1/5$, $(\zeta_0 = 0.349149,\ \zeta_0' = 0.941947)$, and in case (b) $k_x = 1/2$, $(\zeta_0 = 0.872872,\ \zeta_0' = 2.35487)$.

of a shock that moves into an arbitrary superposition of monochromatic rotational and entropic fields.

Motivated by the phenomenon of interference between shock curvature and pre-shock vorticity studied in (Wouchuk *et al.* 2009), and the baroclinic generation analyzed in (Huete Ruiz de Lira *et al.* 2011), we may naturally ask whether that possibility may be exploited to get either a completely irrotational or adiabatic flow downstream. In (Wouchuk *et al.* 2009), the downstream vorticity had two sources: amplification of the pre-shock eddy and shock curvature generated vorticity. Both terms are usually out of phase which leads in general to a reduction of the total downstream vorticity. However, its total value was never found to be zero. We now focus on all the sources of vorticity generation including the vorticity generated by the baroclinic interaction (Huete Ruiz de Lira *et al.* 2011). To be precise, let us consider an upstream array of single mode vorticity written in dimensionless form by:

$$\tilde{\omega}_u = w_u \cos(k_x^{rot} x) \sin(k_y y) \ , \tag{E 1}$$

and an entropic density field given by:

$$\tilde{\rho}_u = \epsilon_u \cos(k_x^{en} x) \cos(k_y y) \ , \tag{E 2}$$

where w_u and ϵ_u are, in principle, arbitrary amplitudes, unlike the re-shock problem. According to the linear theory models of Wouchuk *et al.* (2009), Huete Ruiz de Lira *et al.* (2011) and the model developed in the main article here [see Eq.(2.13)] the downstream vorticity can be shown to be of the form:

$$\tilde{\omega}_d = [\Omega_1 w_u + \Omega_2 p_s^v w_u + \Omega_2 \tilde{p}_s^e \epsilon_u + \Omega_3 \epsilon_k] \cos(Rk_x x) \sin(k_y y) \ , \tag{E 3}$$

where the coefficients $\Omega_1, \Omega_2, \Omega_3$ are formally equivalent to those shown in Eqs.(2.14)-(2.17) respectively, and $\tilde{p}_s^v$, $\tilde{p}_s^e$ are the shock pressure contributions due to the vorticity and entropy fields ahead. We realize that the vorticity downstream would cancel out $(\tilde{\omega}_d = 0)$ if the amplitudes of the upstream modes were correlated in the following way:

$$\frac{\epsilon_u}{w_u} = -\frac{\Omega_1 + \Omega_2 \tilde{p}_s^v}{\Omega_3 + \Omega_2 \tilde{p}_s^e} \ . \tag{E 4}$$

Thus, we can always get a pure irrotational flow even though the fluid ahead is not. From Eqs.(E 3)-(E 4), we can find certain situations in which, the entropic contribution to the downstream vorticity interferes negatively with the total vortical contribution. The minus sign indicates that the phase shift between both contributions has to be $\pi/2$.

For example, for a shock with $M_1 = 3$ moving through air $\gamma = 7/5$ perturbed with a wavelength ratio $k_x/k_y = 1/2$ ($\zeta_0 = 1.04155$), the entropic amplitude divided by the vorticity intensity [Eq.(E 4)] has to be $\epsilon_u/w_u = -1.42978$.

Similarly, we can look for cases in which no entropy perturbations are generated downstream. If we use Eq.(2.27) in the main text, we arrive at:

$$\tilde{\rho}_d^{en} = E_\rho \tilde{p}_s^v w_u + E_\rho \tilde{p}_s^e \epsilon_u + \epsilon_u \ , \tag{E 5}$$

where E_ρ is formally the same as that shown in Eq.(B 56), and it refers to the entropy generation by shock curvature. We realize that the entropic field downstream is zero ($\tilde{\rho}_d^{en} = 0$) if the amplitudes of the modes ahead are correlated in the form:

$$\frac{\epsilon_u}{w_u} = -\frac{E_\rho \tilde{p}_s^v}{1 + E_\rho \tilde{p}_s^e} \ . \tag{E 6}$$

Choosing the same example as before, for a shock with $M_1 = 3$ moving through air $\gamma = 7/5$ and perturbed with a wavelength ratio $k_x/k_y = 1/2$ ($\zeta_0 = 1.04155$), we get $\epsilon_u/w_u = 0.0173194$. Therefore, it is always possible to generate either an irrotational velocity field or a pure adiabatic density perturbation field in the post-shock flow, albeit not in the same situations.

Unfortunately, the re-shock problem does not have this property, because the perturbations generated by the first shock are already correlated, and this correlation can not be modified in order to satisfy either (E 4) or (E 6).

Appendix F. Asymptotic expressions in the strong shocks limit

As shown in the preceding paragraphs, if the shock waves are launched against an isotropic density field, a turbulent velocity, density and acoustic field is generated behind both shocks. The intensity of the perturbations generated downstream depends on the gas compressibility γ, and the shock strengths M_1 and M_1'. To study the compression of a turbulent spectrum we define the statistical averages of the downstream fluctuations after choosing an adequate probability density function. This procedure has been extensively discussed in (Wouchuk *et al.* 2009; Huete Ruiz de Lira *et al.* 2011; Huete *et al.* 2012) and in Section 3 of this article. For the single shock problem, all the averages could be obtained in analytical closed form for any value of the M_1 and γ. Nevertheless, for the re-shock problem considered here, the analytical expressions are cumbersome, and it is in certain limits where the analytical solutions are feasible. As an example, in the strong shocks-limit, and for highly compressible gases the 3D kinetic energy K_{3D} behind the second shock can be expressed as a function of elementary functions. The rotational long wavelength branch ($\zeta_0 < 1$) is:

$$K_{3D}^l \ (M_1 \gg 1, M_1' \gg 1, \gamma - 1 \ll 1) \cong -\frac{1}{2\sqrt{2}} \left[3 \ln\left(\frac{\gamma-1}{2}\right) + 2 \right] (\gamma-1)^{5/2} + \\ + \ \frac{1}{2} \left[\ln\left(\frac{\gamma-1}{2}\right) + \pi \right] (\gamma-1)^3 + O\left[(\gamma-1)^{7/2}\right] \ , \tag{F 1}$$

and the rotational short wavelength contribution is:

$$K_{3D}^s \ (M_1 \gg 1, M_1' \gg 1, \gamma - 1 \ll 1) \cong -\frac{1}{2\sqrt{2}} \left[\ln\left(\frac{\gamma-1}{2}\right) + 2 \right] (\gamma-1)^{5/2} + \\ + \ \frac{1}{2} \left[\ln\left(\frac{\gamma-1}{2}\right) + \pi \right] (\gamma-1)^3 + O\left[(\gamma-1)^{7/2}\right] \ . \tag{F 2}$$

The acoustic part scales as:

$$K_{3D}^{ac}\ (M_1 \gg 1, M_1' \gg 1, \gamma - 1 \ll 1) \cong 2(\gamma-1) - \sqrt{2}\left[\ln\left(\frac{\gamma-1}{2}\right) + 9\right](\gamma-1)^{3/2} + \\ + \quad \left[4\ln\left(\frac{\gamma-1}{2}\right) + 21\right](\gamma-1)^2 - \frac{3}{\sqrt{2}}\left[4\ln\left(\frac{\gamma-1}{2}\right) + 17\right](\gamma-1)^{5/2} + \\ + \quad \left[14\ln\left(\frac{\gamma-1}{2}\right) + \frac{73}{3}\right](\gamma-1)^3 + O\left[(\gamma-1)^{7/2}\right]\ . \tag{F 3}$$

The total kinetic energy is obtained by summing the above equations and can be seen in Eq.(3.16) in the main text. From the above equations, we see that the acoustic part is dominant in that limit. For the vorticity field generated downstream, we can split it up into the long and short wavelength contributions, they are:

$$W_{3D}^{l}\ (M_1 \gg 1, M_1' \gg 1, \gamma - 1 \ll 1) \cong -\frac{2\sqrt{2}}{\sqrt{\gamma-1}}\left[\ln\left(\frac{\gamma-1}{2}\right) + 2\right] + \\ + \quad 4\left[\ln\left(\frac{\gamma-1}{2}\right) + 2\right] - \frac{\sqrt{2}}{3}\left(18\ln\left(\frac{\gamma-1}{2}\right) + 13\right)\sqrt{\gamma-1} + \\ + \quad 2\left[6\ln\left(\frac{\gamma-1}{2}\right) + \frac{13}{3}\right](\gamma-1) + O\left[(\gamma-1)^{3/2}\right]\ , \tag{F 4}$$

$$W_{3D}^{s}\ (M_1 \gg 1, M_1' \gg 1, \gamma - 1 \ll 1) \cong \frac{16}{3(\gamma-1)} - \frac{2\sqrt{2}}{3\sqrt{\gamma-1}}\left[3\ln\left(\frac{\gamma-1}{2}\right) + 28\right] + \\ + \quad 4\ln\left(\frac{\gamma-1}{2}\right) + 37 - \frac{5}{3}\sqrt{2}\left[6\ln\left(\frac{\gamma-1}{2}\right) + 13\right]\sqrt{\gamma-1} + \\ + \quad \left[20\ln\left(\frac{\gamma-1}{2}\right) + 20\right](\gamma-1) + O\left[(\gamma-1)^{3/2}\right]\ , \tag{F 5}$$

where the total vorticity generated behind the second shock is shown in Eq.(3.30). In above expressions Eq.(F 4)-(F 5) we see a divergent behavior when $\gamma \to 1$, which is more important for the short wavelength contribution. Finally, we show the same limits for the different contributions of the density perturbations:

$$G_{3D}^{l}\ (M_1 \gg 1, M_1' \gg 1, \gamma - 1 \ll 1) \cong -\sqrt{2}\left[\ln\left(\frac{\gamma-1}{2}\right) + 2\right](\gamma-1)^{5/2} + \\ + \quad 2\left[\ln\left(\frac{\gamma-1}{2}\right) + 2\right](\gamma-1)^3 + O\left[(\gamma-1)^{7/2}\right]\ , \tag{F 6}$$

$$G_{3D}^{s}\ (M_1 \gg 1, M_1' \gg 1, \gamma - 1 \ll 1) \cong 4(\gamma-1)^2 - \sqrt{2}\left[\ln\left(\frac{\gamma-1}{2}\right) + 12\right](\gamma-1)^{5/2} + \\ + \quad 2\left[\ln\left(\frac{\gamma-1}{2}\right) + 12\right](\gamma-1)^3 + O\left[(\gamma-1)^{7/2}\right]\ , \tag{F 7}$$

the acoustic contribution is:

$$G_{3D}^{ac}\ (M_1 \gg 1, M_1' \gg 1, \gamma - 1 \ll 1) \cong 2(\gamma-1) - \sqrt{2}\left[\ln\left(\frac{\gamma-1}{2}\right) + 9\right](\gamma-1)^{3/2} + \\ + \quad \left[4\ln\left(\frac{\gamma-1}{2}\right) + 21\right](\gamma-1)^2 - \frac{3}{\sqrt{2}}\left[4\ln\left(\frac{\gamma-1}{2}\right) + 17\right](\gamma-1)^{5/2} +$$

$$+ \quad \left[14\ln\left(\frac{\gamma-1}{2}\right)+\frac{73}{3}\right](\gamma-1)^3+O\left[(\gamma-1)^{7/2}\right] \ . \tag{F 8}$$

Now, we show the limits that correspond to the other bound of the curve ($M_1 \gg 1, M_1' \gg 1$), which refer to low compressible gases $\gamma \gg 1$. For the kinetic energy, we separate its components into the long, short for the rotational part, and the acoustic contribution, they are:

$$K_{3D}^{l}(M_1 \gg 1, M_1' \gg 1, \gamma \gg 1) \cong \frac{5}{3\sqrt{2}\gamma^2} - \frac{13}{6\sqrt{2}\gamma^3} + O(\frac{1}{\gamma^4}) \ , \tag{F 9}$$

$$K_{3D}^{s}(M_1 \gg 1, M_1' \gg 1, \gamma \gg 1) \cong \frac{8-5\sqrt{2}}{6\gamma^2} + \frac{49\sqrt{2}-80}{60\gamma^3} + O(\frac{1}{\gamma^4}) \ , \tag{F 10}$$

$$K_{3D}^{ac}(M_1 \gg 1, M_1' \gg 1, \gamma \gg 1) \cong \frac{3-2\sqrt{2}}{5\gamma^2} + \frac{12-8\sqrt{2}}{5\gamma^3} + O(\frac{1}{\gamma^4}) \ . \tag{F 11}$$

We see that all contributions tend to zero as $1/\gamma^2$. The vorticity field generated downstream also tends to zero when $\gamma \gg 1$ as:

$$W_{3D}^{l}(M_1 \gg 1, M_1' \gg 1, \gamma \gg 1) \cong \frac{5}{3\sqrt{2}\gamma^2} - \frac{3}{10\sqrt{2}\gamma^3} + O(\frac{1}{\gamma^4}) \ , \tag{F 12}$$

$$W_{3D}^{s}(M_1 \gg 1, M_1' \gg 1, \gamma \gg 1) \cong \frac{8-5\sqrt{2}}{6\gamma^2} + \frac{48-7\sqrt{2}}{60\gamma^3} + O(\frac{1}{\gamma^4}) \ . \tag{F 13}$$

And finally, the different contributions for the density perturbed field are:

$$G_{3D}^{l}\ (M_1 \gg 1, M_1' \gg 1, \gamma \gg 1) \cong \frac{1}{\sqrt{2}} - \frac{19}{6\sqrt{2}\gamma} + \frac{157}{24\sqrt{2}\gamma^2} - \\ - \quad \frac{4}{3\gamma^{5/2}} - \frac{1247}{240\sqrt{2}\gamma^3} + O(\frac{1}{\gamma^4}) \ , \tag{F 14}$$

$$G_{3D}^{s}\ (M_1 \gg 1, M_1' \gg 1, \gamma \gg 1) \cong 1 - \frac{1}{\sqrt{2}} + \left(\frac{11}{6\sqrt{2}} - \frac{4}{3}\right)\frac{1}{\gamma} + \frac{1888-1633\sqrt{2}}{240\gamma^2} + \\ + \quad \frac{4}{3\gamma^{5/2}} + \frac{4352-5849\sqrt{2}}{480\gamma^3} + O(\frac{1}{\gamma^4}) \ , \tag{F 15}$$

$$G_{3D}^{ac}(M_1 \gg 1, M_1' \gg 1, \gamma \gg 1) \cong \frac{3-2\sqrt{2}}{5\gamma^2} + \frac{12-8\sqrt{2}}{5\gamma^3} + O(\frac{1}{\gamma^4}) \ . \tag{F 16}$$

We observe that for $\gamma \to \infty$, the entropic part $(G_{3D}^{l} + G_{3D}^{s})$ tends to unity, which means that there is no modification over the density perturbations ahead the first shock, and the acoustic part G_{3D}^{ac} tends to zero, because of the low compressibility.

Appendix G. Tables

In this section we have computed some numerical values from the formulas corresponding to the quantities of interest: kinetic energy, acoustic energy flux, vorticity and density generation behind the second shock. These values might be useful as a guide for real or numerical experiments.

M_1	M_1'	K_{2D}	S_{2D}	W_{2D}	G_{2D}
1.001	1.001	0.00172	$8.544 \cdot 10^{-7}$	$7.275 \cdot 10^{-6}$	1.00171
	1.1	0.02742	0.00452	0.01961	1.00938
	2	1.04946	0.11008	2.94877	0.98939
	5	4.34451	0.20684	55.2684	0.74520
	∞	6.48344	0.21305	173.937	0.480379
1.1	1.001	0.02040	$1.178 \cdot 10^{-6}$	0.01961	1.00236
	1.1	0.08915	0.00572	0.09161	1.01386
	2	1.37061	0.13106	4.52099	0.99426
	5	4.25213	0.22965	64.5322	0.75392
	∞	5.58116	0.22240	170.904	0.48939
2	1.001	1.00511	$3.19 \cdot 10^{-6}$	2.95005	0.94511
	1.1	1.32615	0.01646	4.65734	0.97023
	2	2.68148	0.26420	41.9532	0.97902
	5	2.14695	0.30963	276.435	0.77079
	∞	1.97344	0.24435	143.566	0.49071
5	1.001	4.13497	$4.599 \cdot 10^{-6}$	55.3836	0.53253
	1.1	4.48483	0.02518	79.4242	0.55868
	2	5.11074	0.24829	603.273	0.59183
	5	2.79837	0.22450	3585.93	0.47761
	∞	0.38392	0.14516	76.6305	0.28141
∞	1.001	6.16899	$3.914 \cdot 10^{-6}$	174.612	0.15286
	1.1	6.44536	0.02010	246.907	0.17638
	2	6.80979	0.19230	1839.28	0.21599
	5	3.64409	0.10577	10790.4	0.17468
	∞	0.06420	0.04101	22.9294	0.07893

TABLE 1. 2D Downstream kinetic energy average, acoustic energy flux, vorticity and density generation, as a function of M_1 and M_1' for $\gamma = 11/10$.

AZARA, J. L. RODRIGUEZ & EMANUEL, GEORGE 1988 Compressible rotational flows generated by the substitution principle. *Physics of Fluids* **31** (5), 1058–1063.

CLARISSE, JEAN-MARIE, JAOUEN, STÉPHANE & RAVIART, PIERRE-ARNAUD 2004 A godunov-type method in lagrangian coordinates for computing linearly-perturbed planar-symmetric flows of gas dynamics. *Journal of Computational Physics* **198** (1), 80 – 105.

HUETE, C., WOUCHUK, J. G. & VELIKOVICH, A. L. 2012 Analytical linear theory for the interaction of a planar shock wave with a two- or three-dimensional random isotropic acoustic wave field. *Phys. Rev. E* **85**, 026312.

KEVLAHAN, N. K.-R. 1997 The vorticity jump across a shock in a non-uniform flow. *Journal of Fluid Mechanics* **341**, 371–384.

HUETE RUIZ DE LIRA, C., VELIKOVICH, A. L. & WOUCHUK, J. G. 2011 Analytical linear theory for the interaction of a planar shock wave with a two- or three-dimensional random isotropic density field. *Phys. Rev. E* **83** (5), 056320.

MORICE, J. & JAOUEN, S 2003 Perturbations linèaires d'écoulements monodimensionnels à geéometriques plane, cylindrique et sphérique. *CEA-Report. CEA-R-6040 (2003)* **R**, 6040.

VELIKOVICH, A. L., WOUCHUK, J. G., DE LIRA, C. HUETE RUIZ, METZLER, N., ZALESAK,

M_1	M_1'	K_{2D}	S_{2D}	W_{2D}	G_{2D}
1.001	1.001	0.00132	$6.537 \cdot 10^{-7}$	$5.623 \cdot 10^{-6}$	1.00131
	1.1	0.02001	0.00341	0.01401	1.00635
	2	0.52978	0.08154	1.09566	0.90465
	5	1.31445	0.16582	5.44832	0.60516
	∞	1.56731	0.18806	7.92294	0.47731
1.1	1.001	0.01478	$8.621 \cdot 10^{-7}$	0.01401	1.00112
	1.1	0.06243	0.00418	0.06224	1.00847
	2	0.68495	0.09480	1.61920	0.90242
	5	1.35364	0.18427	6.44847	0.60426
	∞	1.40834	0.20149	8.02481	0.48382
2	1.001	0.50560	$1.809 \cdot 10^{-6}$	1.09606	0.88046
	1.1	0.67440	0.00896	1.66141	0.89446
	2	1.35124	0.17415	8.96248	0.80164
	5	1.02777	0.24978	14.6835	0.54264
	∞	0.58462	0.23606	6.83835	0.44506
5	1.001	1.23317	$2.048 \cdot 10^{-6}$	5.45704	0.52271
	1.1	1.39523	0.01054	7.42375	0.53671
	2	1.67421	0.16908	29.5412	0.49206
	5	0.80394	0.19650	37.6771	0.33136
	∞	0.17343	0.15717	3.95791	0.26738
∞	1.001	1.46249	$1.938 \cdot 10^{-6}$	7.94674	0.36921
	1.1	1.60597	0.00975	10.6205	0.38265
	2	1.72394	0.14533	39.9529	0.35588
	5	0.73504	0.15616	48.4198	0.23893
	∞	0.09793	0.11322	2.8283	0.18889

TABLE 2. 2D Downstream kinetic energy average, acoustic energy flux, vorticity and density generation, as a function of M_1 and M_1' for $\gamma = 7/5$.

S. & SCHMITT, A. J. 2007 Shock front distortion and richtmyer-meshkov-type growth caused by a small preshock nonuniformity. *Physics of Plasmas* **14** (7), 072706.

WOUCHUK, J.G. 2001 Growth rate of the linear richtmyer-meshkov instability when a shock is reflected. *Phys. Rev. E* **63** (5), 056303.

WOUCHUK, J.G., HUETE RUIZ DE LIRA, C. & VELIKOVICH, A.L. 2009 Analytical linear theory for the interaction of a planar shock wave with an isotropic turbulent vorticity field. *Phys. Rev. E* **79** (6), 066315.

ZAIDEL', P. M. 1960 Shock wave from a slightly curved piston. *Journal of Applied Mathematics and Mechanics* **24** (2), 316 – 327.

M_1	M_1'	K_{2D}	S_{2D}	W_{2D}	G_{2D}
1.001	1.001	0.00107	$5.292 \cdot 10^{-7}$	$4.502 \cdot 10^{-6}$	1.00106
	1.1	0.01568	0.00273	0.01083	1.00461
	2	0.33940	0.06428	0.59777	0.88527
	5	0.72390	0.13144	1.98978	0.62533
	∞	0.83083	0.14998	2.54823	0.53277
1.1	1.001	0.01152	$6.77 \cdot 10^{-7}$	0.01083	1.00046
	1.1	0.04758	0.00327	0.04650	1.00557
	2	0.43544	0.07353	0.86119	0.88193
	5	0.75133	0.14527	2.32696	0.62398
	∞	0.76118	0.16138	2.59668	0.53861
2	1.001	0.32351	$1.243 \cdot 10^{-6}$	0.59798	0.86936
	1.1	0.43232	0.00605	0.88299	0.87854
	2	0.82174	0.12193	3.59033	0.76757
	5	0.64712	0.19839	4.55824	0.54363
	∞	0.35947	0.19333	2.25990	0.48573
5	1.001	0.67749	$1.323 \cdot 10^{-6}$	1.99261	0.57824
	1.1	0.77845	0.00659	2.63234	0.58746
	2	0.93157	0.11859	7.68411	0.51773
	5	0.48557	0.16689	7.11198	0.36420
	∞	0.14527	0.14706	1.47883	0.32593
∞	1.001	0.77332	$1.275 \cdot 10^{-6}$	2.55502	0.47351
	1.1	0.86530	0.00626	3.31356	0.48252
	2	0.93872	0.10817	9.08250	0.42712
	5	0.43681	0.14531	7.82214	0.29966
	∞	0.10381	0.12339	1.21601	0.26717

TABLE 3. 2D Downstream kinetic energy average, acoustic energy flux, vorticity and density generation, as a function of M_1 and M_1' for $\gamma = 5/3$.

M_1	M_1'	K_{3D}	S_{3D}	W_{3D}	G_{3D}
1.001	1.001	0.00270	$7.642 \cdot 10^{-7}$	$9.699 \cdot 10^{-6}$	1.00269
	1.1	0.03727	0.00250	0.02603	1.01290
	2	1.45082	0.06565	3.83390	0.96782
	5	6.33828	0.16172	74.3317	0.70655
	∞	9.63143	0.17995	236.087	0.44881
1.1	1.001	0.02813	$1.181 \cdot 10^{-7}$	0.02603	1.00376
	1.1	0.12314	0.00371	0.12155	1.01978
	2	1.93346	0.08791	5.91556	0.97299
	5	6.24290	0.19081	86.2304	0.71858
	∞	8.31369	0.19328	232.177	0.46263
2	1.001	1.42561	$3.894 \cdot 10^{-6}$	3.83524	0.94281
	1.1	1.90208	0.01728	6.05336	0.98064
	2	3.92117	0.26773	53.1120	0.97065
	5	3.05516	0.31036	341.553	0.76392
	∞	2.85749	0.23269	192.440	0.47957
5	1.001	6.17114	$6.486 \cdot 10^{-6}$	74.4871	0.53513
	1.1	6.71339	0.03409	106.780	0.57540
	2	7.68855	0.30751	805.641	0.61430
	5	4.13583	0.25580	4756.11	0.50204
	∞	0.47957	0.14372	101.738	0.27999
∞	1.001	9.36522	$5.919 \cdot 10^{-6}$	236.999	0.16333
	1.1	9.79997	0.02991	335.120	0.20003
	2	10.3991	0.27887	2493.15	0.25823
	5	5.54640	0.14066	14587.5	0.21072
	∞	0.06956	0.04294	31.1287	0.08269

TABLE 4. 3D Downstream kinetic energy average, acoustic energy flux, vorticity and density generation, as a function of M_1 and M_1' for $\gamma = 11/10$.

M_1	M_1'	K_{3D}	S_{3D}	W_{3D}	G_{3D}
1.001	1.001	0.00207	$5.846 \cdot 10^{-7}$	$7.417 \cdot 10^{-6}$	1.00206
	1.1	0.02715	0.00186	0.01860	1.00871
	2	0.71952	0.04478	1.41598	0.88198
	5	1.83880	0.11077	7.11246	0.57649
	∞	2.21153	0.13177	10.3996	0.45202
1.1	1.001	0.02034	$8.519 \cdot 10^{-7}$	0.01860	1.00189
	1.1	0.08587	0.00262	0.08263	1.01205
	2	0.94914	0.05801	2.10609	0.87921
	5	1.91451	0.13225	8.45856	0.57691
	∞	1.99994	0.14853	10.6070	0.46286
2	1.001	0.70709	$2.114 \cdot 10^{-6}$	1.4164	0.86955
	1.1	0.95483	0.00847	2.14845	0.89056
	2	1.95412	0.16413	11.4924	0.77542
	5	1.47141	0.23026	18.4987	0.52016
	∞	0.81229	0.20845	9.032	0.43312
5	1.001	1.78276	$2.68 \cdot 10^{-6}$	7.12335	0.51884
	1.1	2.03104	0.01249	9.68974	0.54026
	2	2.47211	0.19473	38.3507	0.48768
	5	1.16635	0.20950	48.4215	0.32512
	∞	0.21877	0.14987	5.18571	0.26358
∞	1.001	2.13573	$2.643 \cdot 10^{-6}$	10.4299	0.37157
	1.1	2.35864	0.01231	13.9384	0.39226
	2	2.56336	0.17768	52.2163	0.36213
	5	1.07720	0.17593	62.8804	0.24061
	∞	0.11751	0.11082	3.72016	0.18887

TABLE 5. 3D Downstream kinetic energy average, acoustic energy flux, vorticity and density generation, as a function of M_1 and M_1' for $\gamma = 7/5$.

M_1	M_1'	K_{3D}	S_{3D}	W_{3D}	G_{3D}
1.001	1.001	0.00167	$4.732 \cdot 10^{-7}$	$6.003 \cdot 10^{-6}$	1.00166
	1.1	0.02126	0.00148	0.01438	1.00630
	2	0.45657	0.03352	0.77211	0.86278
	5	0.99406	0.08054	2.57674	0.59820
	∞	1.14762	0.09548	3.31104	0.50795
1.1	1.001	0.01584	$6.623 \cdot 10^{-7}$	0.01438	1.00089
	1.1	0.06526	0.00201	0.06174	1.00790
	2	0.59718	0.04237	1.11865	0.85898
	5	1.04364	0.09569	3.03029	0.59843
	∞	1.05885	0.10869	3.39821	0.51820
2	1.001	0.44891	$1.41 \cdot 10^{-6}$	0.77234	0.85511
	1.1	0.60727	0.00531	1.14152	0.86885
	2	1.17520	0.10524	4.61673	0.73826
	5	0.91748	0.17284	5.84886	0.51784
	∞	0.49342	0.16076	2.96387	0.47243
5	1.001	0.96468	$1.638 \cdot 10^{-6}$	2.58023	0.56786
	1.1	1.11766	0.00700	3.40862	0.58193
	2	1.35731	0.12263	9.89970	0.50179
	5	0.69518	0.16503	9.11803	0.34868
	∞	0.18831	0.13321	1.92533	0.31861
∞	1.001	1.10957	$1.626 \cdot 10^{-6}$	3.31957	0.46742
	1.1	1.25070	0.00698	4.30479	0.48123
	2	1.37523	0.11693	11.7412	0.41809
	5	0.62853	0.14858	10.0605	0.28947
	∞	0.13154	0.11414	1.58452	0.26275

TABLE 6. 3D Downstream kinetic energy average, acoustic energy flux, vorticity and density generation, as a function of M_1 and M_1' for $\gamma = 5/3$.